JACS
JOURNAL OF THE AMERICAN CHEMICAL SOCIETY
pubs.acs.org/JACS
Article

Accessing Underexplored Biosynthetic Potential by Initiation Unit Engineering of Nonribosomal Peptide Synthetases in *Proteobacteria*

Xianping Bai,[†] Lin Zhong,[†] Yang Liu, Hanna Chen, Xingxing Shi, Xingyan Wang, Ruichen Xu, Qingsheng Yang, Xiaotong Diao, Shengying Li, Dalei Wu, Youming Zhang, Zhiyuan Li, and Xiaoying Bian*

Cite This: *J. Am. Chem. Soc.* 2026, 148, 9114–9129
Read Online
ACCESS | Metrics & More | Article Recommendations | Supporting Information

ABSTRACT: Nonribosomal peptide synthetases (NRPSs) represent a valuable yet underexplored resource for producing bioactive natural products. However, most NRPSs remain silenced potentially due to factors such as dysfunction of the initiation unit. The starter condensation (Cs) domain of the initiation unit catalyzes the lipoinitiation of nonribosomal peptides via the incorporation of an *N*-terminal fatty acyl chain. The concept of initiation unit engineering introduced herein encompasses the replacement of the native initiation unit of NRPSs with a foreign and well-characterized Cs domain-containing initiation unit to activate the NRPS and optimize its expression. This strategy was employed herein to successfully access three of the six previously silent NRPS pathways in *Mycetohabitans rhizoxinica* HKI 454, a bacterium of the class *β-proteobacteria*, resulting in the identification of three classes of lipopeptides. This strategy was then extended to access two NRPS pathways in *Pseudomonas syringae* (*γ-proteobacteria*) and obtain novel lipopeptides, thereby establishing a feasible complement to existing genome mining strategies for natural product discovery. Furthermore, change of the initiation regions of biosynthetic pathways of nonlipidated chitinimide (*β-proteobacteria*) and pseudotetraivprolide (*γ-proteobacteria*) with heterologous Cs-containing initiation units enabled the successful incorporation of fatty acyl chains into the *N*-terminus of both peptide backbones, launching a workable approach to create artificial lipopeptides. Overall, this study provides a practical strategy for the rational recovery of silent BGCs and introduction of fatty acyl chains into nonribosomal peptides, at least in *Proteobacteria*, thereby enriching genome mining and combinatorial biosynthesis approaches for accessing the underexplored biosynthetic potential of NRPSs from various bacteria.

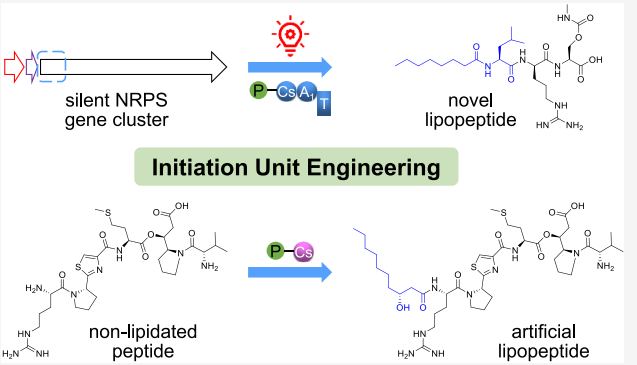

KEYWORDS: *nonribosomal peptide synthetase, initiation unit, starter condensation domain, lipopeptides, combinatorial biosynthesis*

INTRODUCTION

Bacterial natural products (NPs) play a vital role in various fields such as medicine and agriculture owing to their diverse chemical structures and biological activities.[1−3] With the rapid development of genome sequencing technology, a large number of microbial genome sequences have been published.[4−6] Nonetheless, the biosynthetic gene clusters (BGCs) for most bacterial NPs are silent or poorly expressed under standard laboratory conditions.[7,8] Many NPs have hitherto been successfully identified using genome mining strategies,[9−12] including OSMAC (one strain many compounds),[13] promoter insertion,[11,14] overexpression of the regulatory gene,[15] coculture,[16] and heterologous expression.[17−19] However, recent estimates reveal that only approximately 3% of bacterial genomes with the potential to encode NPs have hitherto been characterized.[20] The vast realm of cryptic BGCs represents a valuable source of novel bioactive compounds. However, the likelihood of activating such gene clusters via genome mining strategies remains low.[10]

The lack of success in activating silent BGCs via genome mining strategies may be attributed to an insufficient availability of suitable substrates or dysfunction of the relevant biosynthetic enzymes.[21−24] The initiation module serves as a critical control point that contributes to the overall specificity or functionality of the biosynthetic pathway.[25,26] An inefficient initiation module hampers the efficiency of the entire biosynthetic pathway. If the initiation module is inefficient,

Received: January 18, 2026
Revised: February 6, 2026
Accepted: February 9, 2026
Published: February 18, 2026

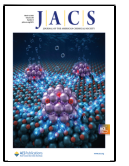

https://doi.org/10.1021/jacs.6c01193
J. Am. Chem. Soc. 2026, 148, 9114−9129

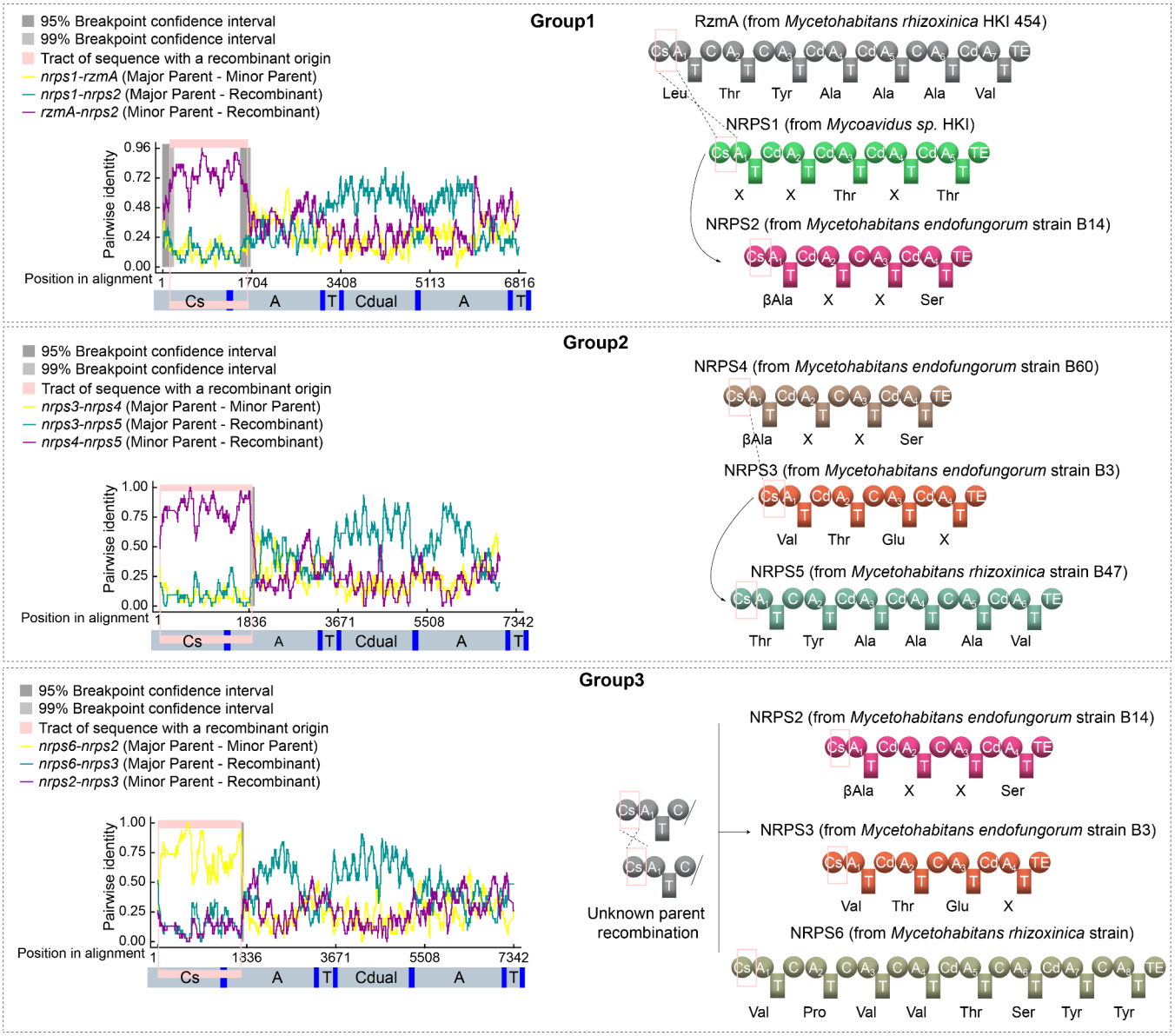

Figure 1. Evolutionary analysis of NRLPs. Groups 1 to 3 exemplify that the initiation module represents a hotspot for recombination. Cs: starter condensation domain, A: adenylation domain; T: thiolation domain; TE: thioesterase domain. C_{dual}: dual condensation/epimerization domain[43] that can change the configuration of upstream amino acid.

then the entire biosynthetic process will not work well. By contrast, an inefficient functioning of the elongation or termination modules may lead to the premature release of the product from the assembly line, which leads to the accumulation of intermediate products. Consequently, streamlining the initiation module of silent biosynthetic pathways may represent a feasible alternative to the current strategy of activating silent BGCs for accessing their biosynthetic potential.

Nonribosomal peptide synthetases (NRPSs) represent the largest class of enzymes that participate in secondary metabolic pathways of bacteria and fungi, and contain initiation, elongation, and termination modules.[5,27] A typical NRPS generally contains three essential domains termed the adenylation (A), thiolation (T) and condensation (C) domains.[25,27] The biosynthesis of nonribosomal lipopeptides (NRLPs), defined by their *N*-terminal acyl chains, is initiated via a dedicated starter condensation (Cs) domain, fatty acyl ligase (AL)/fatty acyl-AMP ligase (FAAL), or polyketide synthases (PKS) modules.[28,29] The Cs domain introduces a fatty acyl chain into the peptide by condensing substrates synthesized by the precursor biosynthetic pathway,[29] which are typically activated by acyl carrier protein (ACP)[30−33] or coenzyme A (CoA).[34−36] AL or FAAL selectively activates free fatty acids, which are then loaded onto ACP or the T domain and transferred to NRPS assembly lines.[37,38] An analysis of distinct biosynthetic pathways reveals that the initiation modules of NRPS mainly consist of A-T, Cs-A-T, or AL/FAAL-A-T architectures. Here, we introduce the concept of the "initiation unit" to describe both the initiation modules and their associated precursor biosynthetic pathways.[29]

Engineering the "initiation unit" of NRPS offers the potential to improve yields, alter the relative proportion of products, and generate new-to-nature peptides. Cheng et al. increased the proportion of polymyxin B1 by exchanging the Cs or A domains to modulate the relative abundance of

https://doi.org/10.1021/jacs.6c01193
J. Am. Chem. Soc. 2026, 148, 9114−9129

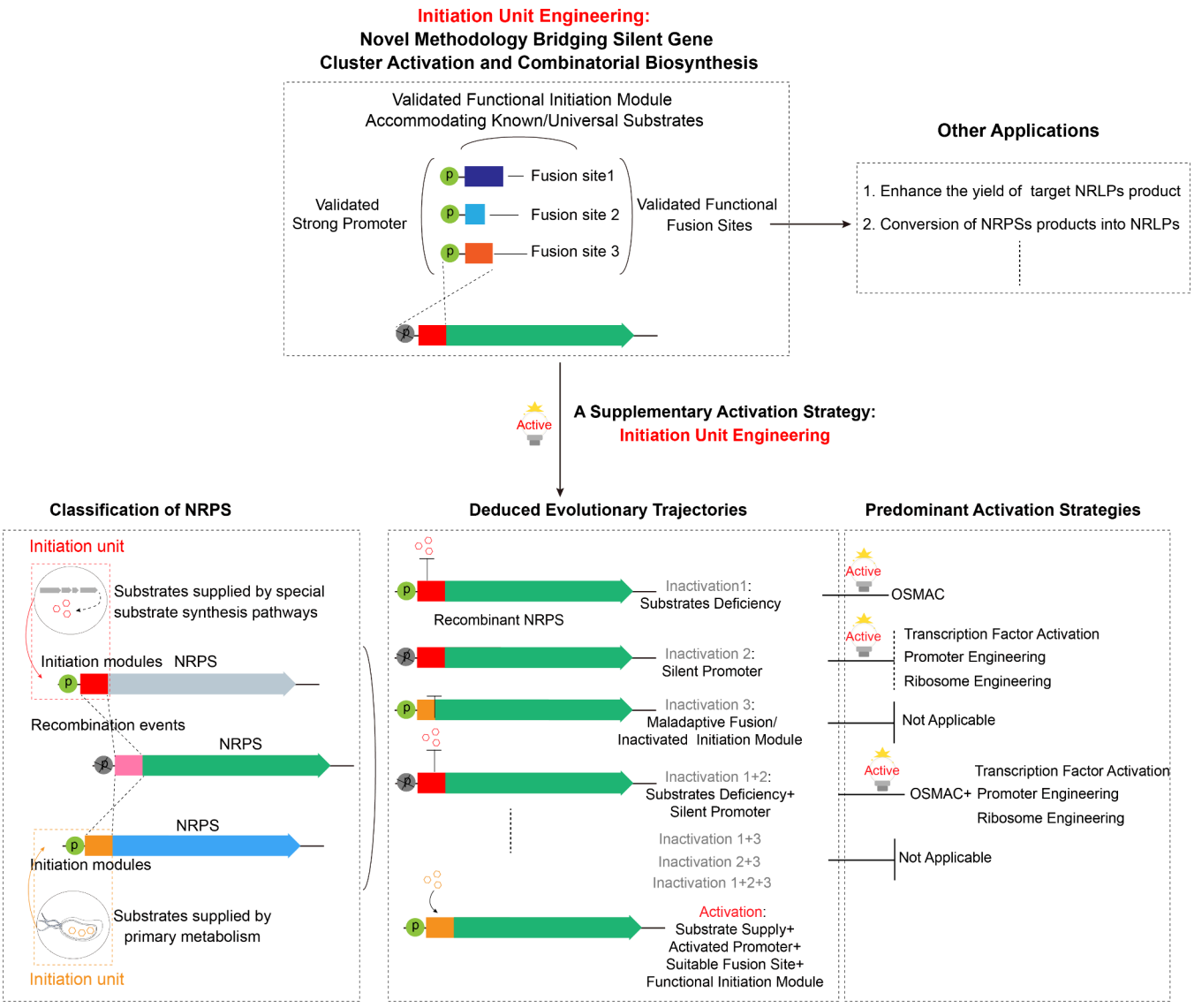

Figure 2. Possible evolutionary pathways and activation strategies of NRPS. Based on these insights, we propose a supplementary activation strategy—"initiation unit engineering". OSMAC: one strain many compounds; P: promoter.

polymyxin analogues.[39] A previous study from our group reported the successfully elucidation of the structure of the complex of RzmA-Cs (R148A) with octanoyl-CoA, and alteration of the length of fatty acid chains of three lipopeptides via Cs-domain swapping, thereby establishing a novel strategy for acyl chain modification.[40] Kang et al. replaced DptE, which loads medium-chain fatty acids, with a heterologous FAAL homologue (HmqF) from *Burkholderia* sp., resulting in the production of high-purity daptomycin.[41]

Engineering strategies targeting the initiation unit have been explored and applied to some extent; nonetheless, genome mining continues to be associated with a high risk of failure. We speculate that this failure is mainly attributable to two factors: (1) inadequate precursor supply and (2) dysfunction of the initiation unit. To address these challenges, an "initiation unit engineering" strategy for activating and optimizing NRPS gene clusters has been introduced herein. This approach employs initiation units that utilize well-known primary metabolites as precursors to replace potentially malfunctioning initiation regions, thereby overcoming the limitations associated with genome mining based on modified regulatory networks and enabling subsequent product optimization to fully exploit the biosynthetic potential of NRPSs.

In the current study, we first examined the possible evolutionary trajectories of NRLPs via bioinformatics analysis of conserved motifs and intermotif sequences of Cs domains across characterized and unknown NRPSs. This analysis enabled us to infer the underlying causes of NRPS inactivation, suggesting the feasibility of "initiation unit engineering". Subsequently, we compared different fusion sites for *in vivo* and *in vitro* modifications of Cs-domain-containing initiation units. Harnessing the identified highly efficient fusion sites, we used a native Cs-containing unit (derived from the same strain) to replace the initiation modules of the endopyrrole biosynthetic pathway (*epy*) and other previously silent NRPS BGCs, leading to the generation of a new lipo-endopyrrole and activation of three gene clusters, respectively. Subsequently, a heterologous Cs domain was employed for replacing the initiation regions of four NRPSs from three phylogenetically distant species, which resulted in the successful activation of these four BGCs and the identification of a new class of lipopeptides. In particular, the addition of a heterologous Cs

https://doi.org/10.1021/jacs.6c01193
J. Am. Chem. Soc. 2026, 148, 9114−9129

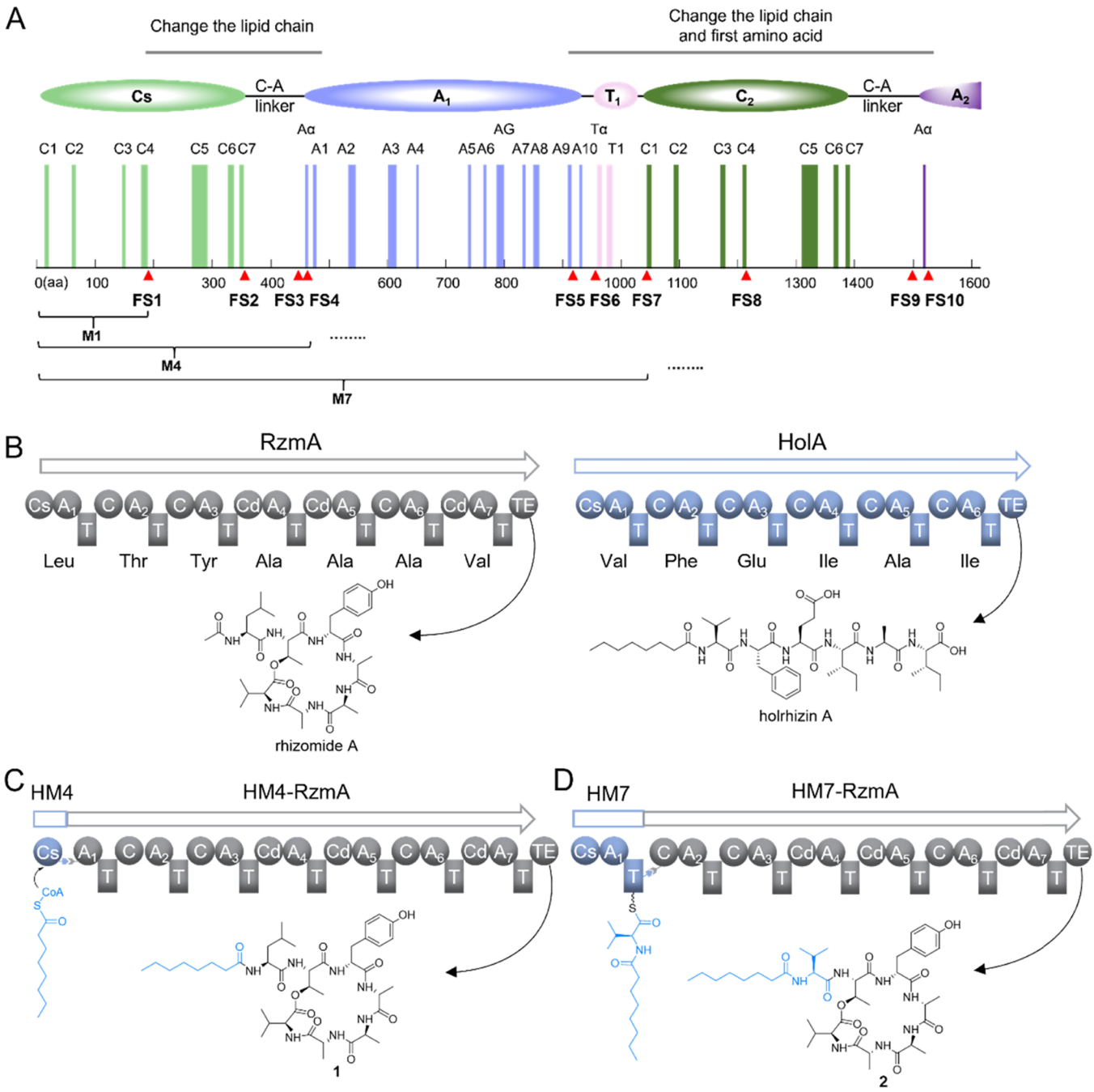

Figure 3. Selection of ten fusion sites within the initiation unit containing the Cs domain. (A) Location of ten FSs and the corresponding initiation regions. The initiation regions of RzmA were annotated using the NRPS Motif Finder. Conserved motifs of the Cs domain and the second C domain are colored light green and dark green, respectively. Conserved motifs of the first A domain are shown in light purple and indicate the positions of the ten sites (FS1−FS10). M1, M4, and M7 denote the initiation modules containing the Cs domains at sites FS1, FS4, and FS7, respectively. (B) The *rzmA* and *holA* gene clusters from *M. rhizoxinica* HKI 454 and their major products, rhizomide A and holrhizin A. Schemes depicting the biosynthesis of recombinant products generated by replacing the initiation region of RzmA with initiation units from HolA, HM4 (lipid chain exchange only, C), and HM7 (exchange of both the lipid chain and first amino acid, D) have been presented as examples.

domain to the initiation region of NRPSs from the chitinimides (*β-proteobacteria*) and pseudotetraivprolide (*γ-proteobacteria*) biosynthetic gene clusters yielded new-to-nature products with an extra fatty acid chain. Thus, the employment of "initiation unit engineering" strategy allowed us to activate and modify silent or underexplored NRPSs and unlocked their biosynthetic potential, providing a feasible strategy of genome mining and combinatorial biosynthesis aimed at discovering and engineering untapped NRPs.

RESULTS AND DISCUSSION

Possible Evolutionary Trajectories of NRLPs

Evolutionary analysis was first employed to identify recombination hotspots across 13 groups comprising 33 NRLP gene clusters.[42] The results revealed that the initiation module is one of the major hotspots for recombination events (Figure 1, Table S5). This suggests that the initiation module and its associated substrate supply may represent critical limiting

https://doi.org/10.1021/jacs.6c01193
J. Am. Chem. Soc. 2026, 148, 9114−9129

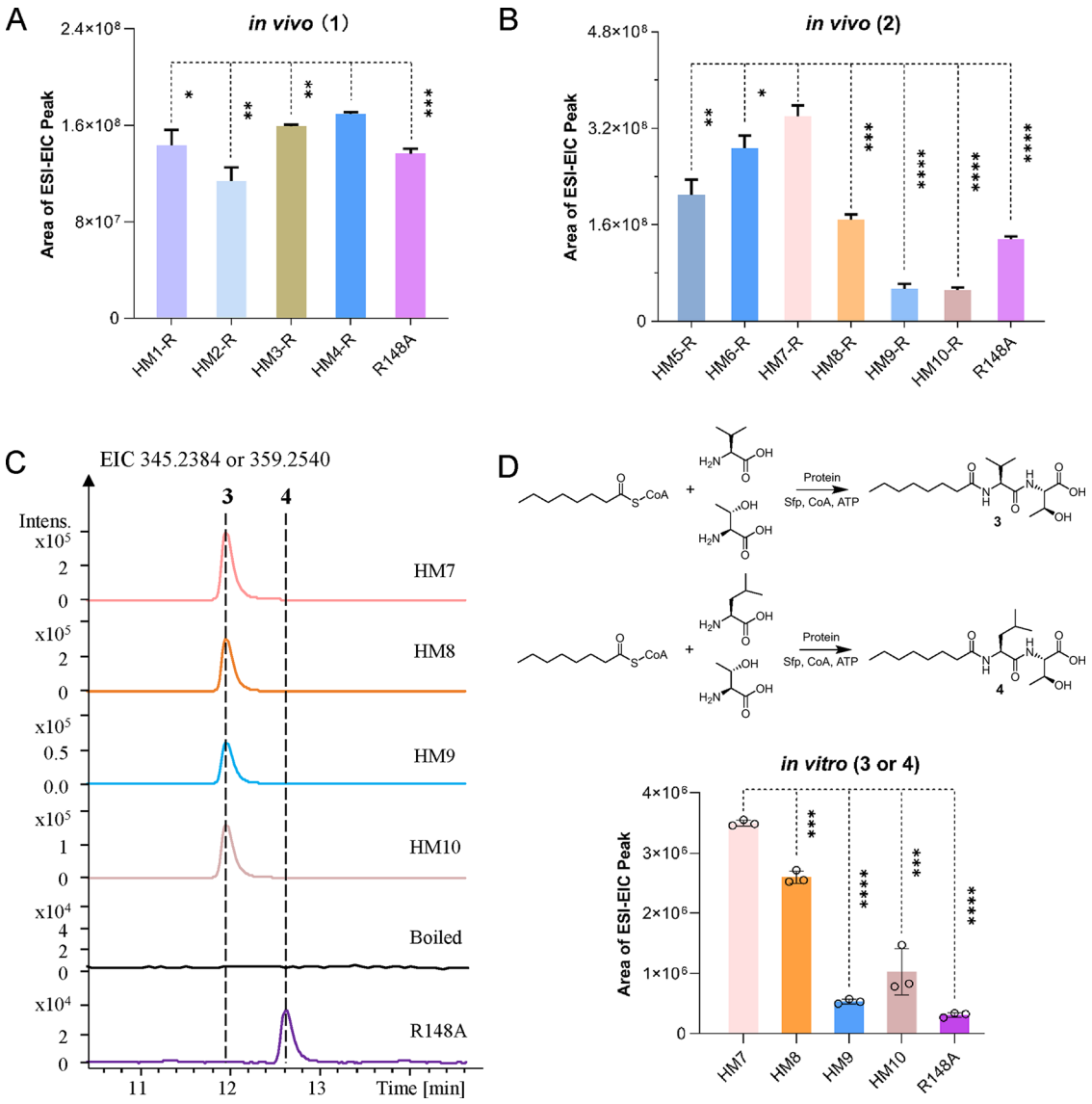

Figure 4. Screening of efficient FSs for initiation of unit exchange. Yields of rhizomide A derivatives **1** (A) and **2** (B) were produced after exchange with different HolA initiation units. R148A denotes RzmA-Cs*, a Cs-domain point mutant (R148A) capable of recognizing octanoyl-CoA (C8-CoA). (C) HPLC analysis of the *in vitro* substrate condensation assay using the fusion proteins HM7−HM10-RzmA (C_2) A_2T_2 and RzmA-Cs*$A_1T_1C_2A_2T_2$ in the presence of ATP, CoA, amino acids, Sfp, Mg^{2+}, and C8-CoA at 30 °C for 3 h. Boiled protein was used as a control. (D) Catalytic activities of wild-type RzmA-Cs*$A_1T_1C_2A_2T_2$ and the fusion proteins. *P* values were calculated using the two-tailed unpaired *t* test. *p < 0.05, **p < 0.01, ***p < 0.001, and ****p < 0.0001, n = 3 independent experiments.

factors for the successful retention of function during the evolution of NRLPs. Based on this observation, the concept of the "initiation unit" within an NRLP biosynthesis gene cluster was proposed herein; this unit encompasses both the initiation module and its corresponding substrate supply pathway.[29]

Inactivation of a natural gene cluster following recombination has been hypothesized herein to arise from one or a combination of the following causes: (1) malfunction of the initiation module, which relies on a specialized substrate supply pathway, thereby hindering access to the required substrate, (2) promoter inactivation, and (3) incompatibility between recombined initiation modules or disruption of their function postfusion (Figure 2). Current mainstream activation strategies for silent gene clusters often fail to address these challenges. The "initiation unit engineering" strategy employed herein offers several key advantages: (1) incorporation of experimentally validated functional initiation modules capable of accepting known or commonly available substrates, (2) integration of strong and experimentally validated promoters, and (3) use of proven fusion sites or exchange units for module recombination. This approach represents a novel methodology that bridges the activation of silent gene clusters with combinatorial biosynthesis (Figure 2).

Poor Activity of Initiation Modules in Silent NRPSs

To test the above hypothesis regarding natural gene cluster inactivation, the initiation module functions of several silent NRPS gene clusters from *Mycetohabitans rhizoxinica* HKI 454 were experimentally characterized herein. Two classes of lipopeptides, rhizomides and holrhizins, were identified from *M. rhizoxinica* HKI 454 in our previous studies using *in situ* insertion of the functional promoters upstream of the core NRPS genes,[44,45] but this method could not be applied to other NRPS BGCs in this strain. To verify the functions of

https://doi.org/10.1021/jacs.6c01193
J. Am. Chem. Soc. 2026, 148, 9114−9129

initiation modules in these silent NRPSs, six NRPS gene clusters designated *2A*, *2C*, *3C*, *5C*, *7C*, and *10C* based on their genomic locations and whose successful activation could not be previously achieved were selected herein (Table S4). These BGCs were directly cloned under the control of constitutive promoters and transferred into heterologous host *Caldimonas brevitalea* DSM 7029[46] (*Burkholderiales*, formerly *Schlegelella brevitalea* DSM 7029) for expression analysis. The results did not reveal any additional detectable peaks compared with the control strain, further confirming that these BGCs are silent or expressed at very low levels under laboratory conditions (Figure S1).

As described above (Figure 2), an inactive initiation module (here, the Cs domain, which is responsible for loading a lipid chain) or the lack of suitable substrates may render the NRPS silent or incapable of synthesizing the corresponding product. To test this hypothesis, the RzmA-Cs domain with a full-length linker was replaced with Cs domains from several silent NRPSs (*2C*, *3C*, *5C*, *epy*, and *10C*) of *M. rhizoxinica*HKI 454. Derivatives were not detectable in the crude extracts (Figure S2), suggesting that NRPS inactivation may be associated with impaired initiation units. The potential reason for this was investigated via sequence alignment of Cs domains from three known and five silent NRPSs of *M. rhizoxinica* HKI 454. The Cs domain contains seven conserved motifs (C1−C7), with the catalytic sequence HHxxxDG located within motif C3.[47,48] The analysis revealed that 2C-Cs, 3C-Cs, 5C-Cs, 7C-Cs, and 10C-Cs harbor residue variations in three (C1, C6, C7), four (C1, C2, C4, C7), one (C5), five (C3−C7), and five (C1−C5) motifs, respectively, suggesting that these substitutions may lead to dysfunction of the corresponding initiation units (Figure S3). Thus, the replacement of the silent initiation unit with well-characterized counterparts may recover initiation module functioning, thereby facilitating the exploration of the biosynthetic potential of these NRPSs.

Screening of Efficient Fusion Sites for Initiation Unit Exchange

Although methods such as exchange units (XU, XUT)[49−51] and module or domain substitution (C-A-T, Cs, A)[32,39,52] have enabled the engineering of certain NRPs, fusion site (FS) compatibility remains a critical factor in NRPS engineering. The identification of optimal FSs for engineering the "initiation unit" responsible for activation was therefore our first endeavor. The "NRPS Motif Finder" platform,[48] which resolves motifs and intermotif structures of NRPS domains, was used for generating a bioinformatics map of the initiation region. Based on sequence alignment, ten conserved FSs (FS1−FS10) were identified and used for defining ten Cs-containing initiation units (M1−M10) for comparative analysis (Figure 3A, Figure S4). These sites include re-engineering points validated in previous studies on NRPS,[40,50,52] with each construct avoiding at least one coevolving sector.[48] The initiation units M1−M10 correspond to CsN (N-lobe, residues 1−188), Cs (with short linker, residues 1−350), CsXU (residues 1−442), Cs (full-length linker, residues 1−479), CsA (with short linker, residues 1−918), CsA (full-length linker, residues 1−958), CsAT (full-length linker, residues 1−1043), $CsATC_2N$ (residues 1−1226), $CsATC_2XU$ (residues 1−1492), and $CsATC_2$ (full-length linker, residues 1−1529). Exchange of the initiation units M1−M4 at FS1−FS4 resulted in the alteration of only the acyl chain (Figure 3C, Figure S4). By contrast, exchange of initiation units M5−M10 at FS5−FS10 led to changes in both the acyl chain and the first amino acid (Figure 3D, Figure S4).

RzmA and HolA, two activated NRPSs from *M. rhizoxinica*, were chosen as templates. Their initiation units use precursors from primary metabolism, and their shared origin with the silent BGCs renders them suitable for "initiation unit engineering". The resulting lipopeptides, rhizomide A and holrhizin A, contain fatty acid chains recognized by the Cs domains of acetyl-CoA (C2-CoA) and octanoyl-CoA (C8-CoA), respectively (Figure 3B). The initiation units M1−M10 of HolA (HM1−HM10) were used to replace the counterparts in RzmA (Figure 3, Figure S5a). The recombinant plasmid was transferred into *E. coli* GB05-MtaA[53] for heterologous expression, and the products were analyzed by high resolution electrospray ionization mass spectroscopy (HRESIMS). The expected products were detected with ten recombinant mutants: compound **1** at *m/z* 816.4834 $[M + H]^+$ (calc. 816.4866) with RzmA-HM1 to RzmA-HM4 and compound **2** at *m/z* 802.4689 $[M + H]^+$ (calc. 802.4709) with RzmA-HM5 to RzmA-HM10, corresponding to the molecular formulas $C_{41}H_{65}N_7O_{10}$ and $C_{40}H_{63}N_7O_{10}$, respectively (Figure 3C, Figure 3D, Figure S17).

Relative quantification analysis revealed that product yields were higher following substitution with HolA initiation units HM4−HM8. Specifically, substitution with the full-length Cs domain (HM4) to alter the acyl chain was more effective than that with HM3 and resulted in slightly higher product yield (Figure 4A). In the scenario with alterations in both the acyl chain and the first amino acid, HM7 afforded the highest yield among all of the test constructs (Figure 4B). Moreover, extending the replacement from the Cs domain to the full-length CsAT module (HM2 to HM7) increased product yields. Further extension to include the C domain of the second C_2-A_2-T_2 module reduced yields, with HM9 and HM10 affording approximately 3-fold lower yields than HM8, whose yield was comparable to that obtained with HM4 (Figure 4A, B). These results reveal that FS4 and FS7 are preferable for initiation of unit engineering strategies depending on the specific objectives.

The recombinants across modules that exhibited significant differences in yields in the *in vivo* experiments, we next expressed and purified two modules from initiation regions: RzmA-Cs*$A_1T_1C_2A_2T_2$ (Cs* is an R148A mutant with recognition of octanoyl- and acetyl-CoA[40]) and four fusion proteins (HM7: HolA-CsA_1T_1-RzmA-$C_2A_2T_2$, HM8: HolA-$CsA_1T_1C_2N$-RzmA-$C_2A_2T_2$, HM9: HolA-$CsA_1T_1C_2XU$-RzmA-A_2T_2, HM10: HolA-$CsA_1T_1C_2$-RzmA-A_2T_2) *in vitro* for yield comparison (Figure S6a). A substrate condensation assay was carried out by incubating the substrates octanoyl-CoA (C8-CoA), L-Leu/L-Val, and L-Thr with the five proteins (Figure 4C). The target product **3** was observed with the four fusion proteins, and the highest yield was obtained with HM7, which is consistent with the *in vivo* results (Figure 4C, Figure 4D, and Figure S6). Compound **4** synthesized by RzmA-Cs*$A_1T_1C_2A_2T_2$ was also detected, but the yield was relatively low.

Verification of Initiation Unit Engineering in *M. rhizoxinica* HKI 454

To evaluate the availability of the screened sites, this strategy was first applied to alter the initiation region of endopyrrole A (*epy*) in *M. rhizoxinica*HKI 454. The pathway is activated upon coculture with the fungal host,[16] suggesting that an insufficient

https://doi.org/10.1021/jacs.6c01193
J. Am. Chem. Soc. 2026, 148, 9114−9129

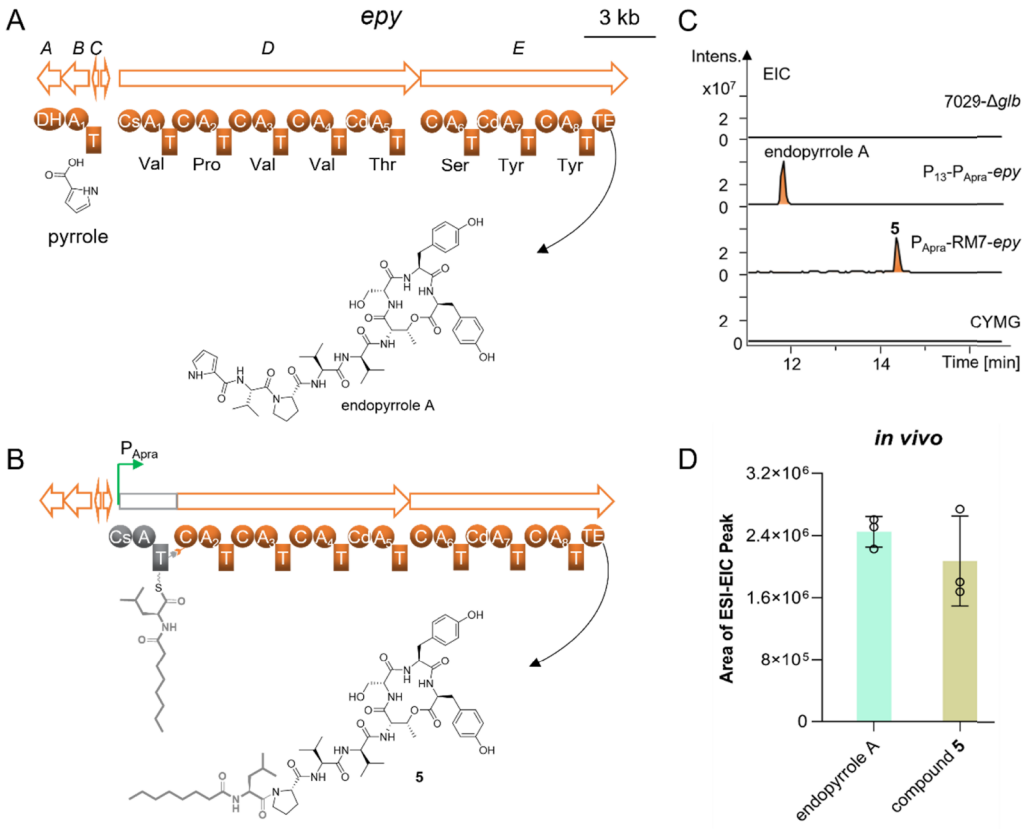

Figure 5. Modification of the initiation module of the BGC *epy* in *M. rhizoxinica* HKI 454. (A) BGC *epy* and its major product, endopyrrole A. (B) Replacement of the initiation module using the fusion site (FS7) of RzmA-Cs*AT to generate compound **5**. (C) HPLC-MS analysis of crude extracts from the heterologous host *C. brevitalea* DSM7029-Δ*glb* expressing *epy* recombinants generated via promoter insertion (P_{13}-P_{Apra}-*epy*) or RM7 replacement (P_{Apra}-RM7-*epy*). Extracted ion chromatograms reveal endopyrrole A at *m/z* 1002.4931 $[M + H]^+$ and compound **5** at *m/z* 1049.5918 $[M + H]^+$. Strain 7029-Δ*glb* (*Caldimonas brevitalea* DSM 7029 with inactivated glidobactin BGC) and CYMG medium served as controls. (D) Comparison of relative yields of derivative **5** and endopyrrole A.

supply of specific pyrrole precursor may be responsible for its silence (Figure 5A). The *epy* BGC was directly cloned under the regulation of the constitutive promoters P_{Apra} and P_{13}[54] to drive expression of the core gene cluster and the gene responsible for the biosynthesis of the specific precursor, respectively (Figure S7). The heterologous expression of the *epy* BGC was successfully accomplished in *C. brevitalea* DSM 7029 Δ*glb* (glidobactin biosynthetic gene cluster inactivated),[46] resulting in the production of endopyrrole A with *m/z* 1001.4858 $[M + H]^+$ (Figure 5C, Figure S7). Next, EpyD-$CsA_{Val}T$ was replaced with RzmA-Cs*$A_{Leu}T$ (RM7) as the new initiation module such that the pyrrole-Val precursor moiety was substituted with an octanoyl-Leu fragment (Figure 5B, Figure 5C).

HPLC-MS analysis revealed a new compound **5**, at *m/z* 1049.5896 $[M + H]^+$ ($C_{54}H_{80}N_8O_{13}$), and a signature fragment at *m/z* 240.1957 $[M + H]^+$ (calcd 240.1958, octanoyl-Leu). MS/MS fragmentation analysis comparison with endopyrrole A indicates that compound **5** is a derivative of endopyrrole A with an *N*-terminal octanoyl chain and Val → Leu substitution (Figure 5B, Figure 5C, and Figure S18). Relative quantification analysis showed that the production efficiency of compound **5** was slightly lower than that of endopyrrole A (Figure 5D). These findings suggest that changing the initiation unit can bypass its dependence on special substrates, underscoring the potential of this strategy for activating silent NRPS pathways.

Changing Initiation Units to Access Silent NRPSs in *M. rhizoxinica* HKI 454

Next, the activation of six silent NRPSs in *M. rhizoxinica* HKI 454 was attempted by applying the selected FSs (Figure 6A and Table S4). Using recombineering,[55] initiation units from RzmA were used for replacing the initiation regions of NRPSs in *M. rhizoxinica* HKI 454 Δ*rhi*, containing inactivated rhizoxin BGC.[44] The specificity of the first A-domain of some NRPSs is unknown; initiation units RM5−RM10, each containing Cs and A domains, were therefore selected herein, with particular emphasis on RM7. The HKI 454 recombinant strains RM7−2A, RM7−2C, RM7−3C, RM8−5C, RM7−7C, and RM8−10C were constructed (Figure S5b, Figure S5c). The C domain in the second module of *10C* is a bifunctional domain (C_{dual}, condensation/epimerization) capable of catalyzing the epimerization of an upstream amino acid. To avoid donor-specific effects, the CsA_1T_1-$C_2A_2T_2$-C_3N region of *10C* was replaced with RM8 ($CsATC_2N$). LC-MS analysis revealed additional peaks in three recombinant strains harboring RM7−2C, RM8−5C, and RM8−10C compared with the control strain (Figure 6B). "Initiation unit engineering" of the directly cloned BGCs *5C* and *10C* and heterologous expression analysis were also carried out (Figure S5b). The results were consistent with those observed in strain HKI 454 (Figure 6B), and the same products were detected, indicating the successful activation of the three silent NRPSs.

https://doi.org/10.1021/jacs.6c01193
J. Am. Chem. Soc. 2026, 148, 9114−9129

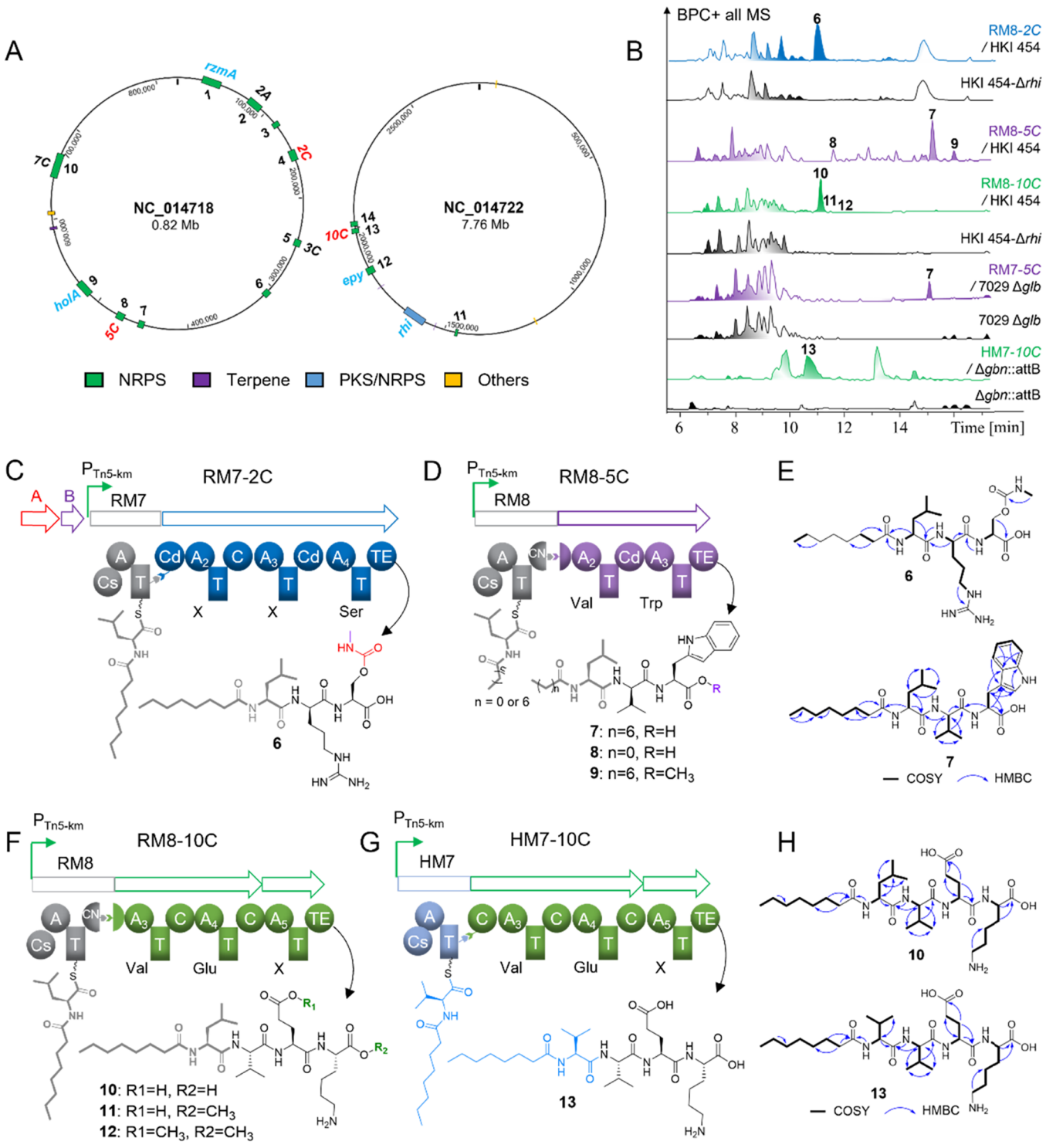

Figure 6. Changing the initiation unit to access previously silent NRPS BGCs in *M. rhizoxinica* HKI 454. (A) Predicted NRPS BGCs in *M. rhizoxinica* HKI 454 using antiSMASH. Previously reported BGCs and the BGCs activated in the current study are shown in blue and red, respectively. (B) HPLC-MS analysis of crude extracts from control strains and recombinant strains obtained by initiation unit exchange. HKI 454-Δ*rhi* denotes a rhizoxin-deficient strain of *M. rhizoxinica*; Δ*gbn*::*attB* : represents the *B. gladioli* Δ*gbn*::*attB* chassis strain used for heterologous expression. Compound **6** was obtained via engineering of the gene cluster *2C* (RM7−2C). Compounds **7**−**9** were obtained from the RM8−5C mutant, whereas **10** and **13** were obtained from strains of RM8−10C and HM7−10C, respectively. Gene cluster *2C* was processed in an independent experimental batch distinct from the other groups. (C) Scheme depicting the biosynthesis of products generated upon modification of gene cluster *2C* with RzmA initiation module RM7. Genes *A* and *B* encode carbamoyltransferase and methyltransferase, respectively. (D) Scheme depicting the biosynthesis of products generated upon modification of the gene cluster*5C* with the RzmA initiation module RM8. (E, H) Key COSY and HMBC correlations of compounds **6**, **7**, **10**, and **13**. Biosynthetic scheme of products generated after modification of the gene cluster *10C* using the RzmA initiation unit RM8 (F) or the HolA initiation unit HM7 (G).

https://doi.org/10.1021/jacs.6c01193
J. Am. Chem. Soc. 2026, 148, 9114−9129

AntiSMASH analysis identified gene cluster *2C*, whose core biosynthetic genes encode four C-A-T modules. Its A_1 and A_4 domains were predicted to activate Ala and Ser, respectively, whereas the substrate specificities of the A_2 and A_3 domains could not be confidently assigned. The mutant strain RM7−2C/HKI 454 Δ*rhi* was constructed based on recombineering at FS7. HPLC−MS analysis of the crude extracts revealed the appearance of a new peak corresponding to compound **6** (Figure 6B). The chemical formula of compound **6** was identified as $C_{25}H_{47}N_7O_7$ at *m*/*z* 558.3626 $[M + H]^+$ (calc. 558.3610) (Figure S19). The ^1H, ^{13}C, DEPT, and HSQC NMR data of **6** (Figures S30−S32, Figure S35, and Table S6) revealed the presence of 25 resolved carbon signals, including 4 methyl (one nitrogenated), 11 methylene (one oxygenated and one nitrogenated), 4 methine (three nitrogenated), and 6 nonprotonated carbons. Further analysis of the HMBC and COSY spectra confirmed that **6** consists of an octanoyl residue, a single Leu, Arg, Ser, and an *N*-methylcarbamoyl group (Figure 6E, Figure S33−S34, and Table S6). The complete sequence octanoyl-Leu^1-Arg^2-Ser^3 was established based on correlations from α-protons and/or α-NH protons to the carbonyl carbons of adjacent residues. However, the precise site of attachment of the *N*-methylcarbamoyl group could not be unambiguously determined due to weak HMBC signals. Gene *A* of BGC *2C* encodes a type III carbamoyltransferase, closely related to TobZ,[56] that catalyzes the ATP-dependent transfer of a carbamoyl group to a hydroxyl acceptor, with subsequent methylation of the resulting carbamoyl moiety mediated by the methyltransferase encoded by gene *B*. The biosynthetic function and common modification patterns of genes *A* and *B* allowed us to propose that this group is linked to the hydroxyl of the Ser.[3] The absolute configurations of the amino acid residues were determined to be L-Leu, D-Arg, and L-Ser based on Marfey's method and C-domain type analysis (Figure 6C, Figure S10).

Compound **6** contains three amino acid residues, whereas gene cluster RM7-*2C* encodes four A domains. $Cd_2A_2T_2$ and $C_3A_3T_3$ were then expressed for conducting *in vitro* adenylation assays[57] for the A domains; both were found to selectively activate Arg (Figure S8a,b). Notably, the Cd_2 is a condensation/epimerization bifunctional domain that converts upstream L-amino acids to the D configuration, whereas Marfey's analysis established an L-Leu residue in compound **6** (Figure S10). Replacement of the 2C−$CsA_1T_1C_2A_2T_2$ with RM7 resulted in HPLC−MS profiles similar to those observed in the RM7−2C mutant (Figure S8c,d). This prompted us to speculate that the module 2 function is skipped during the formation of the tripeptide backbone of compound **6**.

Gene cluster *5C* contains three C-A-T modules starting with a Cs domain. However, the amino acid recognized by the A_1 domain is unknown, while the A_2 and A_3 domains were predicted to recognize Val and Trp, respectively. Four initiation units from RzmA (RM5 and RM7−RM9) were selected for substitution, and the resulting plasmids were transferred into heterologous hosts for product detection. All of the mutant strains produced compounds **7** and **8**, except for the strain harboring RM5−5C (Figure S9a). In addition, a cleaner metabolic background and higher yields were obtained with *Burkholderia gladioli* Δ*gbn::attB*[58] compared to the chassis strain DSM 7029 Δ*glb* (Figure S9b). The products were purified, and structural characterization was carried out by using HRESIMS and NMR spectroscopy. Compound **7** was isolated as a colorless oil, and its molecular formula was established as $C_{30}H_{46}N_4O_5$ with *m*/*z* 543.3519 $[M + H]^+$ (calc. 543.3541) through MS/MS analysis (Figure S20). ^1H, ^{13}C, DEPT, and HSQC NMR analysis of **7** (Figures S36−S38, Figure S41, and Table S7) indicated the presence of 30 resolved carbon signals, which were classified as 5 methyl, 8 methylene, 10 methine (five olefinic and three nitrogenated), and 7 nonprotonated (four carbonyl and three olefinic) carbons. The presence of signals corresponding to four carbonyl (δ_C 173.3−176.6) and three nitrogenated methine (δ_C 53.8−59.5) carbons reveals that **7** may be composed of three amino acid residues and a fatty acid moiety. HMBC correlations indicated that C-31 (the quaternary carbon of the acyl moiety) is connected to Leu C-17 (tertiary carbon); Leu C-30 (quaternary carbon) is connected to Val C-19 (tertiary carbon) as well as Leu C-17 (tertiary carbon); and Val C-28 (quaternary carbon) is connected to Val C-19 (tertiary carbon) and Trp C-18 (tertiary carbon), revealing **7** as the linear lipopeptide octanoyl-Leu^1-Val^2-Trp^3 (Figures S39−S40 and Table S7). The absolute configurations of the amino acid residues were determined to be L-Leu, D-Val, and L-Trp using Marfey's method, in combination with the presence of a dual condensation domain (Figure S10). In addition to compound **7** with an octenyl chain, two derivatives named compounds **8** and **9** with molecular formulas of $C_{24}H_{34}N_4O_5$ and $C_{31}H_{48}N_4O_5$, with *m*/*z* 459.2602 $[M + H]^+$ (calc. 459.2594) and *m*/*z* 557.3674 $[M + H]^+$ (calc. 557.3697), were identified herein, respectively (Figure S20, Tables S7−S9). Compared with compound **7**, **8** contains an acetyl chain in place of the octanoyl chain, whereas **9** features an *O*-methylation Trp residue at the C-terminus (Figures S42−S53).

HRESIMS analysis of the crude extract from RM8-*10C*/HKI 454 Δ*rhi* revealed three additional peaks corresponding to compounds **10**−**12** relative to the control (Figure 6B,F). The molecular formula of **10** was identified as $C_{30}H_{55}N_5O_8$ at *m*/*z* 614.4149 $[M + H]^+$ (calc. 614.4132), with a characteristic fragment ion peak at *m*/*z* 240.1959 $[M + H]^+$ (calc. 240.1958, octanoyl-Leu) (Figure S21). The NMR data of **10** indicated the presence of 30 resolved carbon signals, which were classified as 5 methyl, 13 methylene, 5 methine (four nitrogenated), and 6 nonprotonated carbons (Table S10). Further analysis of NMR spectroscopic data demonstrated that **10** was composed of an octanoyl acid as well as a single Leu, Val, Glu, and a Lys residue (Figures S54−S59). HMBC correlations established the connectivity of the peptide chain: C-27 (acyl quaternary carbon) to Leu 20-NH; Leu C-26 (quaternary) to Val C-23 (tertiary) and Leu C-20 (tertiary); Val C-24 (quaternary) to Glu 22-NH; Glu C-25 (quaternary) to Lys 21-NH; and Lys C-29 (quaternary) to Lys C-21 (tertiary) and C-13(secondary). On the basis of these correlations, compound **10** was established as octanoyl-Leu^1-Val^2-Glu^3-Lys^4 (Figure 6H, Figures S58, and Table S10). The absolute configurations of L-Leu, L-Val, L-Glu, and L-Lys were determined via Marfey's method (Figure S10) and bioinformatics analysis of the C domains. The molecular formulas of **11** and **12** were ascertained to be $C_{31}H_{57}N_5O_8$ and $C_{32}H_{59}N_5O_8$, with *m*/*z* values of 628.4288 $[M + H]^+$ (calc. 628.4280) and 642.4439 $[M + H]^+$ (calc. 614.4436), respectively (Figure 6F, Figure S22), indicating the presence of one (**11**) or two (**12**) more $-CH_2$ groups than **10**. MS/MS fragmentation analysis indicated that **11** contains an *O*-methyl group on the Lys carbonyl, whereas **12** harbors two *O*-methyl groups on the carbonyl of Lys and Glu (Figure S21, Figure

https://doi.org/10.1021/jacs.6c01193
J. Am. Chem. Soc. 2026, 148, 9114−9129

S22). *O*-Methylation of C-terminal residues is not uncommon in *Burkholderiales*[46] and may spontaneously occur during sample preparation using acidified methanol/aqueous solutions via the activities of a specialized TE domain of NPRS[59] or a genome-encoded *O*-methyltransferase.[60]

The A_2 and A_3 domains in 10C are predicted to recognize Val, consistent with the first activated amino acid of HolA (Figure 3B). Accordingly, the initiation region CsAT-C_2AT of 10C was replaced with the HM7 module from HolA for heterologous expression in *B. gladioli* Δ*gbn::attB*. The resulting product **13** was detected in the crude extract at *m*/*z* 600.3978 $[M + H]^+$ (calcd 600.3967, $C_{29}H_{53}N_5O_8$) (Figure 6G, Figure S23). MS/MS analysis revealed a shift in the signature fragment ion peak at *m*/*z* 240.1959 $[M + H]^+$ (octanoyl-Leu) in **10** to *m*/*z* 226.1805 $[M + H]^+$ (octanoyl-Val) in **13** (Figure S23). The ^{1}H, ^{13}C, DEPT, and HSQC NMR analysis of **13** (Figures S60−S62, Figure S65, and Table S11) indicated the presence of 29 resolved carbon signals, which were classified as 5 methyl, 12 methylene, 6 methine (four nitrogenated), and 6 nonprotonated (six carbonyl) carbons. Further analysis of HMBC and COSY correlations involving α-protons and/or α-NH groups with the carbonyl carbons of adjacent residues revealed that **13** corresponds to the linear lipopeptide *N*-octanoyl-Val^1-Val^2-Glu^3-Lys^4 (Figures S63−S64, Table S11). Both **10** and **13** are activated derivatives generated by altering the initiation region of *10C* with well-characterized initiation units from two NRPSs, suggesting that exchange of initiation units is a viable strategy for exploring the potential biosynthetic capacities and structural diversity in NRPs.

The anti-inflammatory activities of four compounds (**7**, **8**, **10**, and **13**) were evaluated herein. Compound **10** exhibited anti-inflammatory activity to a certain extent, and its nitric oxide levels were reduced by 10% at 40 μM relative to the LPS-treated control (Figure S11). None of the compounds exhibited antibacterial activity or cytotoxicity.

Possible Reasons for (Un)Successful Activation

The initiation of the Cs-A-T module in the NRPS is a highly dynamic process. The A_{core} subunit activates the amino acid to form aminoacyl-AMP and subsequently transfers it to the thiol of the 4′-phosphopantetheine (Ppant) arm of the T domain to generate aminoacyl-T (Figure S12). The flexible A_{sub} subunit then swings toward the Cs domain with aminoacyl-T, where the Cs domain condenses the fatty acyl chain with aminoacyl-T to form a peptide bond.[27,61,62] Replacement with heterologous modules often leads to a reduced yield or lack of synthesis of the product, likely due to disruption of essential interdomain interfaces. The highest product yield was observed with HM7, indicating that this design preserves the effective interactions among the C, A, and T domains of the initiation module. Phylogenetic analysis and evolutionary distance calculations of the donor and acceptor Cs domains revealed acceptor Cs domains from the successfully engineered NRPSs with their donor counterparts on the same branch and that they exhibit shorter evolutionary distances than the unsuccessful pairs (Figure S13a). Among the successfully activated NRPSs, 5C-Cs exhibited a short evolutionary distance from the donor RzmA-Cs*, with the highest score (Figure S13b). Understanding dynamic interdomain interactions and selecting native or phylogenetically related initiation units for exchange facilitate efficient NRPS activation and the engineering of lipopeptides with novel structures and bioactivities.

For the remaining three BGCs, various FSs were tested for swapping the initiation regions; however, the desired products were not obtained in any case. Native and engineered initiation units (2A-$A_1T_1C_2A_2T_2$, 3C-Cs$A_1T_1C_2A_2T_2$, 7C-CsA_1-MT-$T_1C_2A_2T_2$, RCs*A_1T_1-2A-$C_2A_2T_2$, RCs*AT-3C-$C_2A_2T_2$, and RCs*A_1T_1-7C-$C_3A_3T_3$) were cloned and expressed in *E. coli* BAP1 to see the reason of the unsuccessful activation by *in vitro* analysis. Constructs RCs*A_1T_1(M7)-2A-$C_2A_2T_2$ and RCs*A_1T_1(M7)-7C-$C_3A_3T_3$ showed higher expression than the original Cs$A_1T_1C_2A_2T_2$, whereas two proteins from the gene cluster *3C* continued to be poorly expressed (Figure S14a), suggesting that the still silence of gene cluster *3C* may be related to limitations in protein expression. Moreover, the proposed dipeptide product could not be detected in *in vitro* assays using RCs*A_1T_1-2A-$C_2A_2T_2$, implying that the fusion may impair domain interactions or module adaptation. *In vitro* assays of RCs*A_1T_1-7C-$C_3A_3T_3$ showed the production of the target product (C8-Leu-Thr) with *m*/*z* 359.2525 $[M + H]^+$ (calc. 359.2540), indicating successful activation of the initiation region (Figure S14d). Thus, the gene cluster *7C* inactivation probably arises from deficiencies in the downstream elongation module.

Using Initiation Unit Engineering to Access Underexplored NRPSs Containing Cs Domains in Other Strains of *Proteobacteria*

The applicability of the "initiation unit engineering" strategy was further explored in other *Burkholderia*-derived NRPSs. Based on antiSMASH analysis, two NRPS BGCs, *Bg*BGC7 and *Bp*BGC12, from *Burkholderia* sp. GL003845 and *Burkholderia plantarii* PG1[63] were selected and predicted to synthesize a pentapeptide and heptapeptide with FA-Thr-Thr-Tyr-X-X and FA-Thr-Pro-Ser-Ala-Ile-X-Pro backbones, respectively (Figure S15a). LC-MS analysis failed to detect the corresponding products, indicating that both BGCs were silent under laboratory conditions. The A_1 domains from *Bg*BGC7 and *Bp*BGC12 are predicted to recognize Thr. In our previous study, two classes of lipopeptides, burriogladiodins (*bgdd*) and haereogladiodins (*hgdd*), were mined from *Burkholderia gladioli* ATCC 10248,[64] also start with Thr, which was subsequently dehydrated to dehydrobutyrine (Dhb), possibly catalyzed by the downstream C-domain.[26] The initiation units of *Bg*BGC7 and *Bp*BGC12 were altered herein with the Cs domains from Hgdd and Bgdd using FS4, respectively (Figure S15b, Figure S15d). The recombinant plasmids were transformed into DSM 7029 Δ*glb* and *B. gladioli* Δ*gbn::attB* for heterologous expression; extra peaks (compounds **14**−**15** and **16**−**19**) were observed in the crude extracts from strains HM4-*Bg*BGC7 and BM4-*Bp*BGC12, suggestive of the activation of the previously silent biosynthesis pathways *Bg*BGC7 and *Bp*BGC12. The substrate prediction of A domains combined with HRESIMS analysis allowed us to determine that the products of HM4-*Bg*BGC7 are haereogladiodin B (**14**) and A (**15**)[64] and the products of BM4-*Bp*BGC12 are burrioglumin A (**16**)[65] and three new derivatives, burrioglumin C-E (**17**−**19**) (Figure S15c,d, Figure S24−S25). These results suggest that the "initiation unit engineering" strategy can be extended to phylogenetically related *Burkholderia*-derived NRPSs.

Nonribosomal lipopeptides are abundant secondary metabolites in *Pseudomonas* strains.[66] The "initiation unit engineering" strategy was therefore applied for investigating two NRPSs (*Ps*BGC10 and *Ps*BGC9A) of *Pseudomonas syringae* 1.3070.

https://doi.org/10.1021/jacs.6c01193
J. Am. Chem. Soc. 2026, 148, 9114−9129

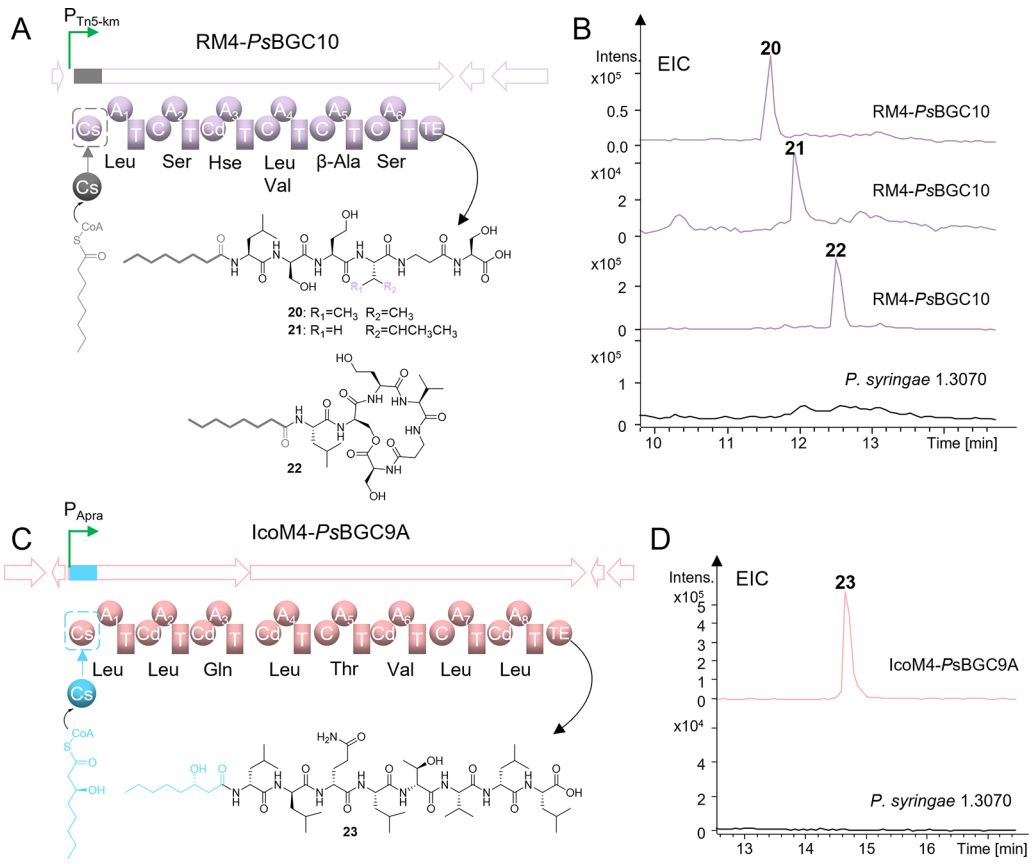

Figure 7. Engineering the initiation unit to access underexplored gene clusters in *Pseudomonas syringae* 1.3070. (A, C) Scheme depicting product biosynthesis following the engineering of *Ps*BGC10 with RzmA-Cs* (RM4) and *Ps*BGC9A with Ico-Cs (IcoM4). (B, D) HPLC-MS analysis of the crude extracts of wild-type *P. syringae* 1.3070 and the recombinant strains obtained upon *Ps*BGC10 and *Ps*BGC9A initiation unit exchanged. Extracted ion chromatograms (EIC) are shown at *m/z* 703.4236 $[M + H]^+$ (**20**), *m/z* 717.4393 $[M + H]^+$ (**21**), *m/z* 685.4131 $[M + H]^+$ (**22**), and *m/z* 1054.7122 $[M + H]^+$ (**23**).

Sequence alignment identified several substitutions at conserved motifs in the Cs domains of *Ps*BGC10 and *Ps*BGC9A. In *Ps*BGC10, the conserved Glu residue in the C1 motif is replaced by Gly (which has a substantially different structure and physicochemical property), and the conserved Gln residue in the C6 motif is substituted with Glu (Figure S16). In *Ps*BGC9A, the conserved nonpolar Leu residue in the C2 motif is replaced by the polar residue Thr, and the conserved Met in the C5 motif is replaced by His. These substitutions at highly conserved positions may be associated with the compromised performance of the initiation region. AntiSMASH analysis indicated that *Ps*BGC10 and *Ps*BGC9A encode six and eight C-A-T modules, corresponding to the structural scaffolds FA−Leu−Ser−X−X−*β*-Ala−Ser and FA−X−Leu−Gln−-Leu−Thr−Val−Leu−Leu, respectively. Detailed substrate predictions by PARAS suggested that the A_3 and A_4 domains of *Ps*BGC10 recognize homoserine (Hse) and Leu/Val, respectively, whereas the A_1 domain of *Ps*BGC9A is likely specific for Leu/Ile. Using double crossover recombination, the native Cs domains of *Ps*BGC10 and *Ps*BGC9A were successfully substituted with the RzmA-Cs* (RM4) and Ico-Cs (Ico-M4, the first Cs domain of the icosalide biosynthetic pathway in *B. gladioli* ATCC 10248[67]), respectively (Figure 7A,C). HPLC-MS and MS/MS analysis of the crude extracts enabled the detection and identification of the products of RM4-*Ps*BGC10 to be **20**−**22** and the product of IcoM4-*Ps*BGC9A to be **23**, a derivative of syringafactin A[66] (Figure 7, Figures S26−S27). These results indicate the efficacy of the initiation unit engineering strategy for accessing the *Proteobacteria*-derived NRPSs and redirecting the assembly of nonribosomal lipopeptides while preserving the integrity of the core peptide scaffold.

Creating Artificial Lipopeptides by Heterologous Initiation Unit Exchange

Lipid chains are critical determinants of NRP bioactivity.[28,66] The fatty-acid moiety anchors the lipopeptides to the phospholipid bilayer, thereby prolonging target engagement,[68,69] while chain length modulates the balance between biological activity and cytotoxicity.[70] Initiation unit engineering provides a strategy for enhancing yields while concomitantly converting nonlipidated NRPs into lipopeptides. The addition of a fatty acyl chain at the *N*-terminus of NRPs, achieved via the introduction of a Cs-containing initiation unit, can alter its chemical properties and enhance its biological activity and drug-like potential.

In our previous study, heterologous expression of a cryptic *chm* BGC from *Chitinimonas koreensis* DSM 17726 (family *Burkholderiaceae*) in *C. brevitalea* DSM 7029 resulted in the discovery of novel NRPs called chitinimides.[46] ChmA catalyzes the formation of a ureido-bond between the first Phe and the second Dhb in charge of the fragment in a head-to-head manner via the first ureido-bond-forming C_u domain (Figure 8A). To add an *N*-terminal lipid chain, the native A_{Phe}-T-C_u initiation region was replaced with a Cs-containing initiation

https://doi.org/10.1021/jacs.6c01193
J. Am. Chem. Soc. 2026, 148, 9114−9129

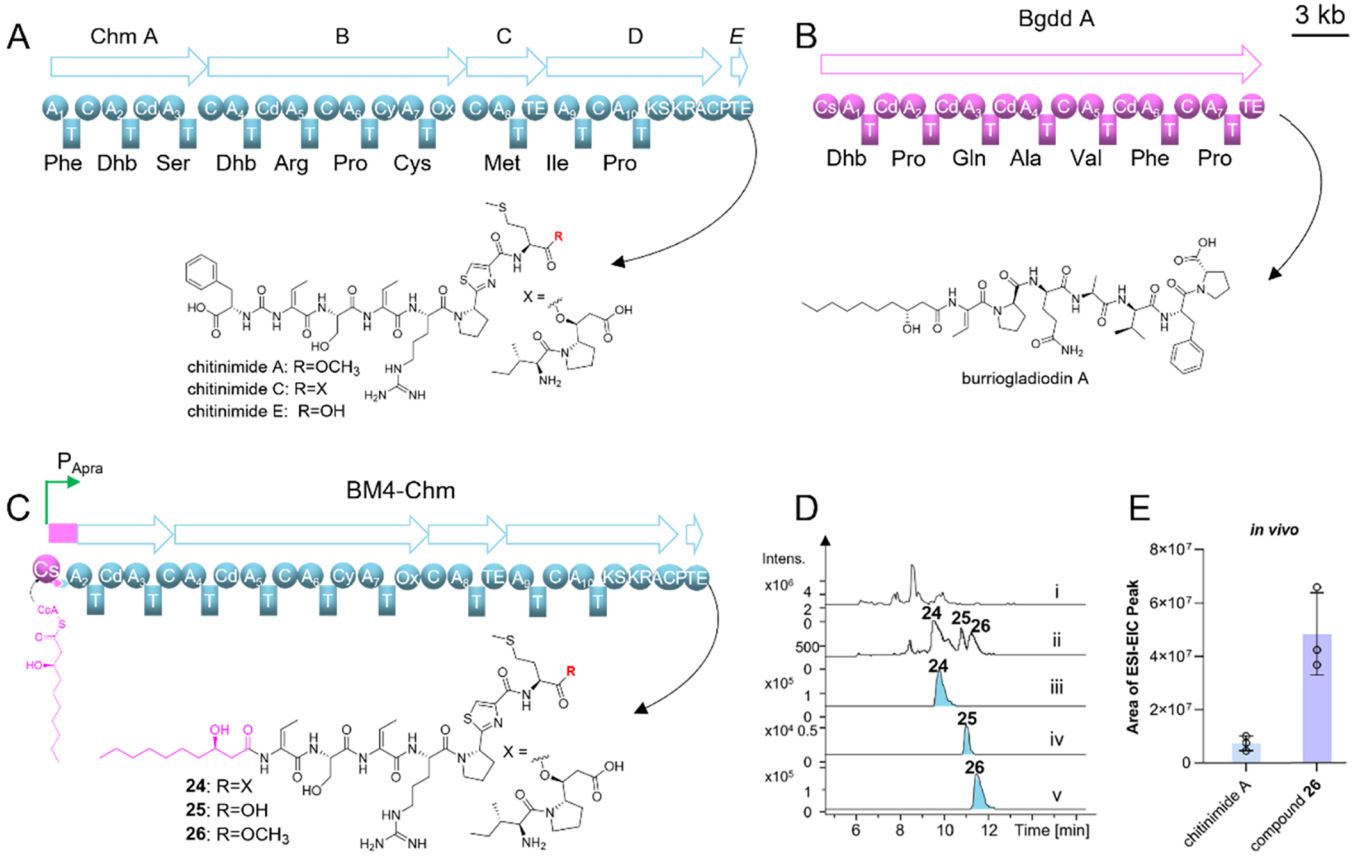

Figure 8. Introduction of an *N*-terminal fatty acyl chain by engineering the initiation region of ChmA. (A, B) Schematic representation of the BGCs *bgdd* and *chm* from *B. gladioli* ATCC 10248 and *C. koreensis* DSM 17726, respectively, and their major products, burriogladiodin A and chitinimide A, C, and E. (C) Scheme depicting the biosynthesis of products obtained upon engineering BGC *chm* with the Bgdd-derived initiation unit BM4. (D) UV spectra (254 nm, ii) and HPLC-MS analysis of crude extracts from strain DSM 7029Δ*glb*/BM4-*chm*. Base peak chromatograms are shown at *m/z* 1163.5951 $[M + H]^+$ (**24**), *m/z* 909.4321 $[M + H]^+$ (**25**), and *m/z* 923.4478 $[M + H]^+$ (**26**). (E) Comparison of relative yields of derivative **26** and chitinimide A.

unit that preferentially loads Dhb, thereby preventing ureido bond formation and improving compatibility between the exogenous Cs and target NRPS. This Cs domain was selected due to the Dhb residue in the lipopeptide burriogladiodin (*bgdd*) from *B. gladioli* ATCC 10248[64] and integration via the optimized fusion site FS4 (Figure 8B,C). The engineered *chm* BGC plasmid (BM4-*chm*) was integrated into the genome of *C. brevitalea* DSM 7029 Δ*glb* for subsequent fermentation and product detection.

Metabolic profiling of the crude extract revealed three distinct absorption peaks at 254 nm, corresponding to products **24**, **25**, and **26**, with compound **26** exhibiting the highest yield (Figure 8D). HRESIMS analysis determined the molecular formula of **26** as $C_{41}H_{66}N_{10}O_{10}S_2$ with *m/z* 923.4473 $[M + H]^+$ (calc. 923.4478) (Figure S28). Detailed NMR analysis in combination with MS/MS data showed that **26** consists of a *β*-hydroxydecanoate chain and seven amino acid residues (Dhb, L-Ser, Dhb, L-Arg, L-Pro, L-Cys, and L-Met), representing a derivative of lipo-chitinimide A (Figures S66−S71, Table S12). HRESIMS and MS/MS analysis further indicated that **24** ($C_{53}H_{86}N_{12}O_{13}S_2$, at *m/z* 582.3033 $[M + 2H]^{2+}$, calc. 582.3012) and **25** ($C_{40}H_{64}N_{10}O_{10}S_2$, at *m/z* 909.4319 $[M + H]^+$, calc. 909.4321) are lipidated derivatives of chitinimides C and E, respectively (Figure 8C, Figure S28). The yield of the engineered compound **26** was nearly 5-fold higher than that of chitinimide A (Figure 8E), underscoring the potential of this engineering approach for facilitating scalable production. Cytotoxicity assays showed that **25** exhibited moderate cytotoxicity against the cell lines of HepG2 and A549 tumors, with IC_{50} values of 8.36 and 12.02 *μ*M, respectively, surpassing those of **24** and **26** as well as chitinimide A (Table S13). Due to its extremely low yield, chitinimide E could not be purified for comparative evaluation.

The BGC *pip* responsible for pseudotetraivprolide synthesis has been recently identified and activated in *Pseudomonas*.[71] Its biosynthesis begins with an A domain (Arg) but lacks a Cs domain (Figure 9A), and this BGC is also found in *P. syringae* 1.3070 (*Ps*BGC6). Using double crossover recombination, the Cs domains (P_{Apra}-BM4, Bgdd-Cs) were added upstream of the A_1 domain of PipA (Figure 9B). This modification resulted in the addition of a fatty acyl chain at the *N*-terminal of pseudotetraivprolide to yield derivative **27** (Figure 9C), with a molecular formula of $C_{41}H_{69}N_9O_9S_2$ at *m/z* 448.7430 $[M + 2H]^{2+}$ (calc. 448.7403), and the structure was verified by MS/MS fragmentation analysis (Figure 9C, Figure S29).

Cs domains play a crucial role in loading lipid chains during the biosynthesis of nonribosomal lipopeptides and display variability in the properties of substrate selection and specificity across various NRPS BGCs. Some recognize and condense a single fatty acyl substrate from primary metabolism or with different modifications, whereas others exhibit substrate-tolerance and the ability to synthesize diverse lipid

https://doi.org/10.1021/jacs.6c01193
J. Am. Chem. Soc. 2026, 148, 9114−9129

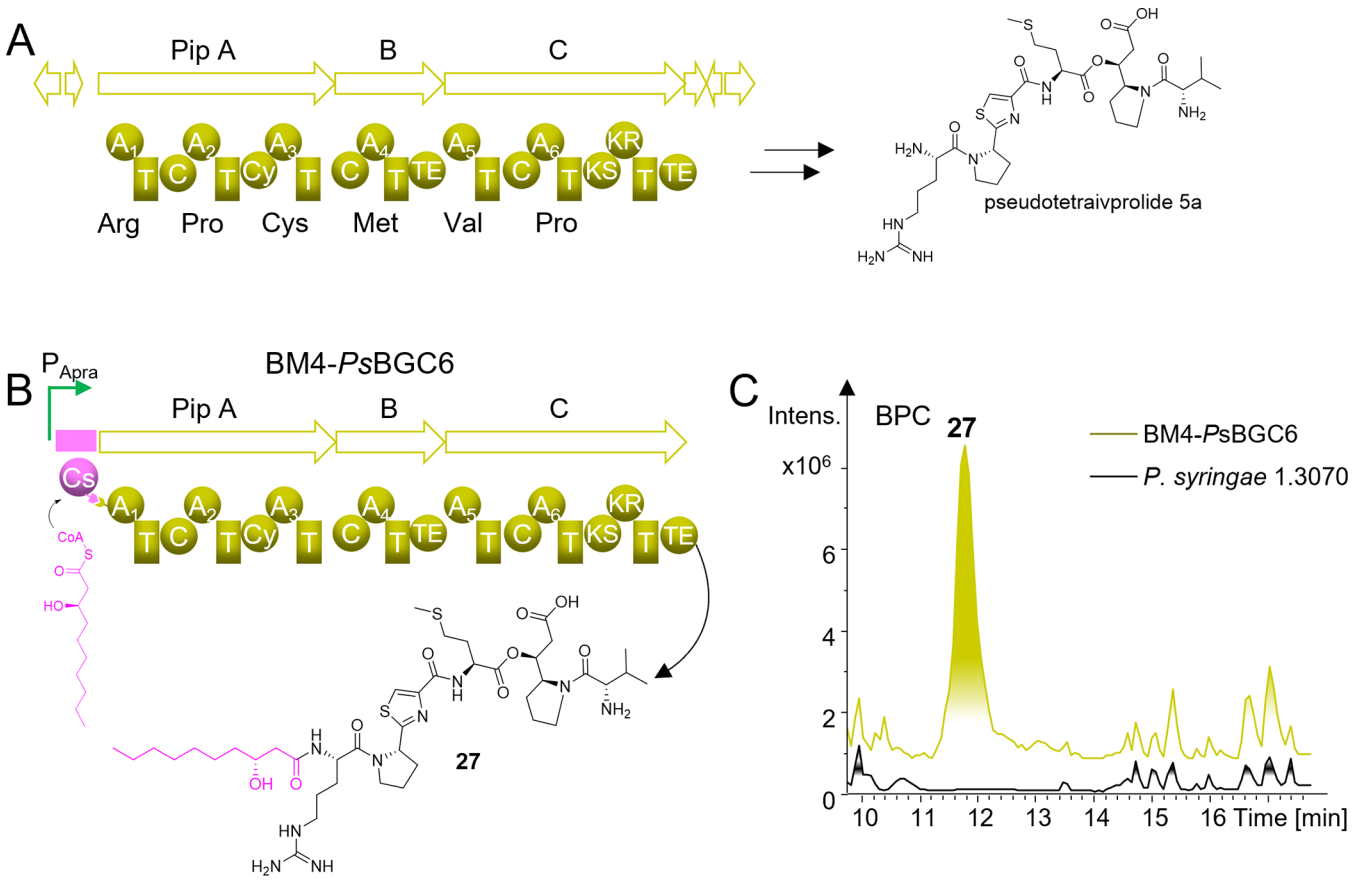

Figure 9. Introduction of an *N*-terminal fatty acyl chain in pseudotetraivprolide via engineering of the initiation region of PipA. (A) Schematic representation of BGC *pip* and its product pseudotetraivprolide **5a** from *Pseudomonas*. (B) Scheme depicting the biosynthesis of product **27** following the addition of Bgdd-Cs (BM4) to PipA. (C) HPLC-MS analysis of crude extracts from *P. syringae* 13070 mutants generated upon the insertion of P_{Apra}-BM4.

chains.[33,72,73] Recent studies have increasingly focused on Cs domain engineering approaches for modulating its selectivity toward lipid chain substrates.[39,40,74] Our study showcases the incorporation of lipid chains into the typically nonlipidated chitinimides and pseudotetraivprolides derived from *β*- and *γ*-*Proteobacteria* to generate non-natural lipopeptides, providing a new perspective for NRPS engineering and optimizing.

SUMMARY

This study introduces the concept that the engineering initiation unit can activate and optimize the expression of silent or underexplored NRPS, successfully accessing three previously silent NRPSs pathways in a *Burkholderiales* strain. Furthermore, the application of this strategy to previously unexplored NRPSs of *Proteobacteria* resulted in the activation of four BGCs, yielding derivatives and a class of new lipopeptides. This strategy provides a feasible complement to the current genome mining approaches. The initiation unit engineering strategy integrates the principles of both gene cluster activation and combinatorial biosynthesis. This method enables the revival of NRPS BGCs in a manner in which existing regulation-based genome mining strategies cannot readily be achieved. Moreover, *N*-terminal lipid chains are crucial for the activity of lipopeptides. To enhance the properties of NRPs lacking these lipid chains, a heterologous initiation unit was employed for replacing or supplementing the original initiation region, thereby facilitating the creation of artificial nonribosomal lipopeptides and ultimately yielding four novel lipo-derivatives. This study presents an effective approach for achieving the activation and optimization of nonribosomal peptides and offers profound insight into the exploration of bacterial biosynthetic pathways.

METHODS

A detailed description of the methods mentioned in the text—including bacterial strains, reagents and growth conditions, plasmid construction, bioinformatics analysis, the design and replacement of the initiation unit, *in situ* modification of the initiation units of NRPS in *M. rhizoxinica* HKI 454, fermentation and subsequent HPLC-MS analysis of crude extracts from various strains, purification and characterization of compounds, Marfey's analysis, biological activity screening and purification, sequence alignment and distance analysis, and characterization of enzymes—are provided in the Supporting Information.

ASSOCIATED CONTENT

Supporting Information

The Supporting Information is available free of charge at https://pubs.acs.org/doi/10.1021/jacs.6c01193.

Bacterial strains, mutants, plasmids, primers, and gene clusters used in the study (Tables S1−S4); Evolutionary analysis of 13 groups containing 33 NRLP gene clusters in this study (Tables S5); The ^{1}H (600 MHz), ^{13}C NMR (150 MHz), HMBC, and COSY data of compounds in this study (Tables S6−S12); IC_{50} values of compounds **24**−**26** using seven cancer cell lines in

https://doi.org/10.1021/jacs.6c01193
J. Am. Chem. Soc. 2026, 148, 9114−9129

Tables S13; Multiple alignment of the NRPS initiation module (Figure S3, Figure S4, and Figure S16); Workflow diagram of direct cloning (Figure S1), heterologous expression and modification of initiation module of BGCs in this study (Figure S5, Figure S7, and Figure S15); Functional validation of the initiation module of the silent BGCs in *M. rhizoxinica* HKI 454 (Figure S2), *in vitro* analysis yields compound **3** and compound **4** (Figure S6), comparison the yields of compound **8** (Figure S9), evaluation of the anti-inflammatory activities of compounds **7**, **8**, **10**,and **13** (Figure S11); Marfey's analysis of the amino acid constituents of various compounds (Figure S10). *In vitro* adenylation assays of 2C-$C_2A_2T_2$ and 2C-$C_3A_3T_3$ and *in vitro* protein expression and functional characterization of silent NRPSs (Figure S8, Figure S14); HRESIMS spectra and MS/MS fragmentation data of products (Figures S17−S29); NMR spectra of compounds used in this study (Figures S30−S71) (PDF)

AUTHOR INFORMATION

Corresponding Author

Xiaoying Bian − *Helmholtz International Lab for Anti-Infectives, State Key Laboratory of Microbial Technology, Shandong University, Qingdao, Shandong 266237, China;* orcid.org/0000-0002-1356-3211; Email: bianxiaoying@sdu.edu.cn

Authors

Xianping Bai − *Helmholtz International Lab for Anti-Infectives, State Key Laboratory of Microbial Technology, Shandong University, Qingdao, Shandong 266237, China*

Lin Zhong − *State Key Laboratory of Microbial Technology (Changde R&D Base), Institute of Synthetic Biology Industry, Hunan University of Arts and Science, Changde, Hunan 415000, China;* orcid.org/0000-0002-2636-4430

Yang Liu − *Helmholtz International Lab for Anti-Infectives, State Key Laboratory of Microbial Technology, Shandong University, Qingdao, Shandong 266237, China*

Hanna Chen − *College of Pharmacy, Linyi University, Linyi 276000, China*

Xingxing Shi − *Helmholtz International Lab for Anti-Infectives, State Key Laboratory of Microbial Technology, Shandong University, Qingdao, Shandong 266237, China*

Xingyan Wang − *Helmholtz International Lab for Anti-Infectives, State Key Laboratory of Microbial Technology, Shandong University, Qingdao, Shandong 266237, China*

Ruichen Xu − *Center for Quantitative Biology, Academy for Advanced Interdisciplinary Studies, Peking University, Beijing 100871, China*

Qingsheng Yang − *Helmholtz International Lab for Anti-Infectives, State Key Laboratory of Microbial Technology, Shandong University, Qingdao, Shandong 266237, China*

Xiaotong Diao − *Helmholtz International Lab for Anti-Infectives, State Key Laboratory of Microbial Technology, Shandong University, Qingdao, Shandong 266237, China*

Shengying Li − *Helmholtz International Lab for Anti-Infectives, State Key Laboratory of Microbial Technology, Shandong University, Qingdao, Shandong 266237, China;* orcid.org/0000-0002-5244-870X

Dalei Wu − *Helmholtz International Lab for Anti-Infectives, State Key Laboratory of Microbial Technology, Shandong University, Qingdao, Shandong 266237, China;* orcid.org/0000-0003-1817-7229

Youming Zhang − *Helmholtz International Lab for Anti-Infectives, State Key Laboratory of Microbial Technology, Shandong University, Qingdao, Shandong 266237, China*

Zhiyuan Li − *Center for Quantitative Biology, Academy for Advanced Interdisciplinary Studies, Peking University, Beijing 100871, China;* orcid.org/0000-0001-6662-2636

Complete contact information is available at: https://pubs.acs.org/10.1021/jacs.6c01193

Author Contributions

†X.B. and L.Z. contributed equally to this work.

Notes

The authors declare no competing financial interest.

ACKNOWLEDGMENTS

We thank Guannan Lin, Zhifeng Li, Jingyao Qu, Jing Zhu, Haiyan Sui, and Xiangmei Ren from the State Key Laboratory of Microbial Technology of Shandong University for help and guidance in HRMS, NMR, and LC. This work was supported by National Natural Science Foundation of China (32570094, 32201195), the Key R&D Program of Shandong Province, China (2025CXPT191), Fundamental Research Funds of Shandong University (2023QNTD001), Young Talent Development Program (M2025YA03), and Frontiers and Challenges Project (SKLMTFCP-2023-05) and Open Projects Fund (M2024-05) of SKLMT.

REFERENCES

(1) Hegemann, J. D.; Birkelbach, J.; Walesch, S.; Müller, R. Current Developments in Antibiotic Discovery: Global Microbial Diversity as a Source for Evolutionary Optimized Anti-bacterials. *EMBO Rep.* **2023**, *24*, No. e56184.

(2) Shakya, A. K.; Naik, R. R.; Al-Obaidi, J. The Chemotherapeutic Potentials of Compounds Isolated from the Plant, Marine, Fungus, and Microorganism: Their Mechanism of Action and Prospects. *J. Trop. Med.* **2022**, *2022*, 1.

(3) Atanasov, A. G.; Zotchev, S. B.; Dirsch, V. M.; Supuran, C. T. Natural Products in Drug Discovery: Advances and Opportunities. *Nat. Rev. Drug Discov.* **2021**, *20*, 200−216.

(4) Blin, K.; Shaw, S.; Augustijn, H. E.; Reitz, Z. L.; Biermann, F.; Alanjary, M.; Fetter, A.; Terlouw, B. R.; Metcalf, W. W.; Helfrich, E. J. N.; van Wezel, G. P.; Medema, M. H.; Weber, T. antiSMASH 7.0: New and Improved Predictions for Detection, Regulation, Chemical Structures and Visualisation. *Nucleic Acids Res.* **2023**, *51* (W1), W46−W50.

(5) Kautsar, S. A.; Blin, K.; Shaw, S.; Weber, T.; Medema, M. H. BiG-FAM: The Biosynthetic Gene Cluster Families Database. *Nucleic Acids Res.* **2021**, *49* (D1), D490−D497.

(6) Cimermancic, P.; Medema, M. H.; Claesen, J.; Kurita, K.; Wieland Brown, L. C.; Mavrommatis, K.; Pati, A.; Godfrey, P. A.; Koehrsen, M.; Clardy, J.; Birren, B. W.; Takano, E.; Sali, A.; Linington, R. G.; Fischbach, M. A. Insights into Secondary Metabolism from a Global Analysis of Prokaryotic Biosynthetic Gene Clusters. *Cell.* **2014**, *158* (2), 412−421.

(7) Zhang, X.; Hindra; Elliot, M. A. Unlocking the Trove of Metabolic Treasures: Activating Silent Biosynthetic Gene Clusters in Bacteria and Fungi. *Curr. Opin. Microbiol.* **2019**, *51*, 9−15.

(8) Scherlach, K.; Hertweck, C. Mining and Unearthing Hidden Biosynthetic Potential. *Nat. Commun.* **2021**, *12* (1), 3864.

(9) Chevrette, M. G.; Gavrilidou, A.; Mantri, S.; Selem-Mojica, N.; Ziemert, N.; Barona-Gómez, F. The Confluence of Big Data and Evolutionary Genome Mining for the Discovery of Natural Products. *Nat. Prod. Rep.* **2021**, *38* (11), 2024−2040.

(10) Bauman, K. D.; Butler, K. S.; Moore, B. S.; Chekan, J. R. Genome Mining Methods to Discover Bioactive Natural Products. *Nat. Prod. Rep.* **2021**, *38* (11), 2100−2129.
(11) Baral, B.; Akhgari, A.; Metsä-Ketelä, M. Activation of Microbial Secondary Metabolic Pathways: Avenues and Challenges. *Synth. Syst. Biotechnol.* **2018**, *3* (3), 163−178.
(12) Li, L. Next-generation synthetic biology approaches for the accelerated discovery of microbial natural products. *Eng Microbiol.* **2023**, *3* (1), No. 100060.
(13) Pan, R.; Bai, X.; Chen, J.; Zhang, H.; Wang, H. Exploring Structural Diversity of Microbe Secondary Metabolites Using OSMAC Strategy: A Literature Review. *Front. Microbiol.* **2019**, *10*, 294.
(14) Montiel, D.; Kang, H. S.; Chang, F. Y.; Charlop-Powers, Z.; Brady, S. F. Yeast Homologous Recombination-Based Promoter Engineering for the Activation of Silent Natural Product Biosynthetic Gene Clusters. *Proc. Natl. Acad. Sci. U.S.A.* **2015**, *112* (29), 8953−8958.
(15) Wang, B.; Guo, F.; Dong, S. H.; Zhao, H. Activation of Silent Biosynthetic Gene Clusters Using Transcription Factor Decoys. *Nat. Chem. Biol.* **2019**, *15* (2), 111−114.
(16) Niehs, S. P.; Dose, B.; Scherlach, K.; Pidot, S. J.; Stinear, T. P.; Hertweck, C. Genome Mining Reveals Endopyrroles from a Nonribosomal Peptide Assembly Line Triggered in Fungal−Bacterial Symbiosis. *ACS Chem. Biol.* **2019**, *14* (8), 1811−1818.
(17) Komatsu, M.; Uchiyama, T.; Ōmura, S.; Cane, D. E.; Ikeda, H. Genome-Minimized Streptomyces Host for the Heterologous Expression of Secondary Metabolism. *Proc. Natl. Acad. Sci. U.S.A.* **2010**, *107* (6), 2646−2651.
(18) Ke, J.; Yoshikuni, Y. Multi-Chassis Engineering for Heterologous Production of Microbial Natural Products. *Curr. Opin. Biotechnol.* **2020**, *62*, 88−97.
(19) Huo, L.; Hug, J. J.; Fu, C.; Bian, X.; Zhang, Y.; Müller, R. Heterologous Expression of Bacterial Natural Product Biosynthetic Pathways. *Nat. Prod. Rep.* **2019**, *36* (10), 1412−1436.
(20) Gavriilidou, A.; Kautsar, S. A.; Zaburannyi, N.; Krug, D.; Müller, R.; Medema, M. H.; Ziemert, N. Compendium of Specialized Metabolite Biosynthetic Diversity Encoded in Bacterial Genomes. *Nat. Microbiol.* **2022**, *7* (5), 726−735.
(21) Mao, D.; Yoshimura, A.; Wang, R.; Seyedsayamdost, M. R. Reporter-Guided Transposon Mutant Selection for Activation of Silent Gene Clusters in *Burkholderia Thailandensis*. *ChemBioChem* **2020**, *21* (13), 1826−1831.
(22) Covington, B. C.; Xu, F.; Seyedsayamdost, M. R. A Natural Product Chemist's Guide to Unlocking Silent Biosynthetic Gene Clusters. *Annu. Rev. Biochem.* **2021**, *90* (1), 763−788.
(23) Liu, Z.; Zhao, Y.; Huang, C.; Luo, Y. Recent Advances in Silent Gene Cluster Activation in *Streptomyces*. *Front. Bioeng. Biotechnol.* **2021**, *9*, No. 632230.
(24) Stasiak, M.; Maćkiw, E.; Kowalska, J.; Kucharek, K.; Postupolski, J. Silent Genes: Antimicrobial Resistance and Antibiotic Production. *Pol. J. Microbiol.* **2021**, *70* (4), 421−429.
(25) Fischbach, M. A.; Walsh, C. T. Assembly-Line Enzymology for Polyketide and Nonribosomal Peptide Antibiotics: Logic, Machinery, and Mechanisms. *Chem. Rev.* **2006**, *106* (8), 3468−3496.
(26) Dekimpe, S.; Masschelein, J. Beyond Peptide Bond Formation: The Versatile Role of Condensation Domains in Natural Product Biosynthesis. *Nat. Prod. Rep.* **2021**, *38* (10), 1910−1937.
(27) Süssmuth, R. D.; Mainz, A. Nonribosomal Peptide Synthesis—Principles and Prospects. *Angew. Chem., Int. Ed.* **2017**, *56* (14), 3770−3821.
(28) Chooi, Y.-H.; Tang, Y. Adding the Lipo to Lipopeptides: Do More with Less. *Chem. Biol.* **2010**, *17* (8), 791−793.
(29) Zhong, L.; Boopathi, S.; Wang, X.; Chen, H.; Bai, X.; Shi, X.; Yang, Q.; Bian, X.; Zhang, Y. Expanding the Horizon of Natural Products: The Role of Starter Units in Nonribosomal Lipopeptide Biosynthesis. *ACS Synth. Biol.* **2025**, *14* (5), 1336−1351.
(30) Kraas, F. I.; Giessen, T. W.; Marahiel, M. A. Exploring the Mechanism of Lipid Transfer during Biosynthesis of the Acidic Lipopeptide Antibiotic CDA. *FEBS Lett.* **2012**, *586* (3), 283−288.
(31) Alexander, D. C.; Rock, J.; Gu, J. Q.; Mascio, C.; Chu, M.; Brian, P.; Baltz, R. H. Production of Novel Lipopeptide Antibiotics Related to A54145 by Streptomyces Fradiae Mutants Blocked in Biosynthesis of Modified Amino Acids and Assignment of lptJ, lptK and lptL Gene Functions. *J. Antibiot.* **2011**, *64* (1), 79−87.
(32) Nguyen, K. T.; Ritz, D.; Gu, J.-Q.; Alexander, D.; Chu, M.; Miao, V.; Brian, P.; Baltz, R. H. Combinatorial Biosynthesis of Novel Antibiotics Related to Daptomycin. *Proc. NatI. Acad. Sci. U.S.A.* **2006**, *103* (46), 17462−17467.
(33) Baltz, R. H. Genome Mining for Drug Discovery: Cyclic Lipopeptides Related to Daptomycin. *J. Ind. Microbiol. Biotechnol.* **2021**, *48* (3−4), No. kuab020.
(34) Kraas, F. I.; Helmetag, V.; Wittmann, M.; Strieker, M.; Marahiel, M. A. Functional Dissection of Surfactin Synthetase Initiation Module Reveals Insights into the Mechanism of Lipoinitiation. *Chem. Biol.* **2010**, *17* (8), 872−880.
(35) Wang, C.; Flemming, C. J.; Cheng, Y.-Q. Discovery and Activity Profiling of Thailandepsins A through F, Potent Histone Deacetylase Inhibitors, from *Burkholderia Thailandensis* E264. *Med. Chem. Comm.* **2012**, *3* (8), 976−981.
(36) Chen, H.; Zhong, L.; Zhou, H.; Bai, X.; Sun, T.; Wang, X.; Zhao, Y.; Ji, X.; Tu, Q.; Zhang, Y.; Bian, X. Biosynthesis and Engineering of the Nonribosomal Peptides with a C-Terminal Putrescine. *Nat. Commun.* **2023**, *14* (1), 6619.
(37) Chen, H.; Zhong, L.; Zhou, H.; Sun, T.; Zhong, G.; Tu, Q.; Zhuang, Y.; Bai, X.; Wang, X.; Xu, J.; Xia, L.; Shen, Y.; Zhang, Y.; Bian, X. Biosynthesis of Glidomides and Elucidation of Different Mechanisms for Formation of β-OH Amino Acid Building Blocks. *Angew. Chem., Int. Ed.* **2022**, *61* (35), No. e202203591.
(38) Hansen, D. B.; Bumpus, S. B.; Aron, Z. D.; Kelleher, N. L.; Walsh, C. T. The Loading Module of Mycosubtilin: An Adenylation Domain with Fatty Acid Selectivity. *J. Am. Chem. Soc.* **2007**, *129* (20), 6366−6367.
(39) Yuan, Y.; Xu, Q. M.; Yu, S. C.; Sun, H. Z.; Cheng, J. S.; Yuan, Y. J. Control of the Polymyxin Analog Ratio by Domain Swapping in the Nonribosomal Peptide Synthetase of *Paenibacillus Polymyxa*. *J. Ind. Microbiol. Biotechnol.* **2020**, *47* (6−7), 551−562.
(40) Zhong, L.; Diao, X.; Zhang, N.; Li, F.; Zhou, H.; Chen, H.; Bai, X.; Ren, X.; Zhang, Y.; Wu, D.; Bian, X. Engineering and Elucidation of the Lipoinitiation Process in Nonribosomal Peptide Biosynthesis. *Nat. Commun.* **2021**, *12* (1), 296.
(41) Ji, C. H.; Park, S.; Lee, K.; Je, H. W.; Kang, H. S. Lipidation Engineering in Daptomycin Biosynthesis. *J. Am. Chem. Soc.* **2024**, *146* (44), 30434−30442.
(42) Martin, D. P.; Varsani, A.; Roumagnac, P.; Botha, G.; Maslamoney, S.; Schwab, T.; Kelz, Z.; Kumar, V.; Murrell, B. RDP5: a computer program for analyzing recombination in, and removing signals of recombination from, nucleotide sequence datasets. *Virus Evol.* **2021**, *7* (1), veaa087.
(43) Balibar, C. J.; Vaillancourt, F. H.; Walsh, C. T. Generation of D Amino Acid Residues in Assembly of Arthrofactin by Dual Condensation/Epimerization Domains. *Chem Biol.* **2005**, *12* (11), 1189−1200.
(44) Wang, X.; Zhou, H.; Chen, H.; Jing, X.; Zheng, W.; Li, R.; Sun, T.; Liu, J.; Fu, J.; Huo, L.; Li, Y. z.; Shen, Y.; Ding, X.; Müller, R.; Bian, X.; Zhang, Y. Discovery of Recombinases Enables Genome Mining of Cryptic Biosynthetic Gene Clusters in *Burkholderiales* Species. *Proc. Natl. Acad. Sci. U.S.A.* **2018**, *115* (18), E4255−E4263.
(45) Chen, H.; Zhou, H.; Sun, T.; Xu, J.; Tu, Q.; Yang, J.; Zhang, Y.; Bian, X. Identification of Holrhizins E−Q Reveals the Diversity of Nonribosomal Lipopeptides in Paraburkholderia Rhizoxinica. *J. Nat. Prod.* **2020**, *83* (2), 537−541.
(46) Liu, J.; Zhou, H.; Yang, Z.; Wang, X.; Chen, H.; Zhong, L.; Zheng, W.; Niu, W.; Wang, S.; Ren, X.; Zhong, G.; Wang, Y.; Ding, X.; Müller, R.; Zhang, Y.; Bian, X. Rational Construction of Genome-Reduced *Burkholderiales* Chassis Facilitates Efficient Heterologous

https://doi.org/10.1021/jacs.6c01193
J. Am. Chem. Soc. 2026, 148, 9114−9129

Production of Natural Products from Proteobacteria. *Nat. Commun.* **2021**, *12* (1), 4347.
(47) Konz, D.; Marahiel, M. A. How do peptide synthetases generate structural diversity? *Chem Biol.* **1999**, *6* (2), R39−R48.
(48) He, R.; Zhang, J.; Shao, Y.; Gu, S.; Song, C.; Qian, L.; Yin, W.-B.; Li, Z. Knowledge-Guided Data Mining on the Standardized Architecture of NRPS: Subtypes, Novel Motifs, and Sequence Entanglements. *PLoS Comput. Biol.* **2023**, *19* (5), No. e1011100.
(49) Bozhüyük, K. A. J.; Präve, L.; Kegler, C.; Schenk, L.; Kaiser, S.; Schelhas, C.; Shi, Y. N.; Kuttenlochner, W.; Schreiber, M.; Kandler, J.; Alanjary, M.; Mohiuddin, T. M.; Groll, M.; Hochberg, G. K. A.; Bode, H. B. Evolution-Inspired Engineering of Nonribosomal Peptide Synthetases. *Science* **2024**, *383* (6689), No. eadg4320.
(50) Bozhüyük, K. A. J.; Fleischhacker, F.; Linck, A.; Wesche, F.; Tietze, A.; Niesert, C.-P.; Bode, H. B. De Novo Design and Engineering of Non-Ribosomal Peptide Synthetases. *Nat. Chem.* **2018**, *10* (3), 275−281.
(51) Bozhüyük, K. A. J.; Linck, A.; Tietze, A.; Kranz, J.; Wesche, F.; Nowak, S.; Fleischhacker, F.; Shi, Y.-N.; Grün, P.; Bode, H. B. Modification and de Novo Design of Non-Ribosomal Peptide Synthetases Using Specific Assembly Points within Condensation Domains. *Nat. Chem.* **2019**, *11* (7), 653−661.
(52) Calcott, M. J.; Owen, J. G.; Ackerley, D. F. Efficient Rational Modification of Non-Ribosomal Peptides by Adenylation Domain Substitution. *Nat. Commun.* **2020**, *11* (1), 4554.
(53) Bian, X.; Huang, F.; Stewart, F. A.; Xia, L.; Zhang, Y.; Müller, R. Direct Cloning, Genetic Engineering, and Heterologous Expression of the Syringolin Biosynthetic Gene Cluster in E. Coli through Red/ET Recombineering. *ChemBioChem* **2012**, *13* (13), 1946−1952.
(54) Ouyang, Q.; Wang, X.; Zhang, N.; Zhong, L.; Liu, J.; Ding, X.; Zhang, Y.; Bian, X. Promoter Screening Facilitates Heterologous Production of Complex Secondary Metabolites in *Burkholderiales* Strains. *ACS Synth. Biol.* **2020**, *9* (2), 457−460.
(55) Yin, J.; Zheng, W.; Gao, Y.; Jiang, C.; Shi, H.; Diao, X.; Li, S.; Chen, H.; Wang, H.; Li, R.; Li, A.; Xia, L.; Yin, Y.; Stewart, A. F.; Zhang, Y.; Fu, J. Single-Stranded DNA-Binding Protein and Exogenous RecBCD Inhibitors Enhance Phage-Derived Homologous Recombination in *Pseudomonas*. *iScience* **2019**, *14*, 1−14.
(56) Wei, J.; Zhang, X.; Zhou, Y.; Cheng, X.; Lin, Z.; Tang, M.; Zheng, J.; Wang, B.; Kang, Q.; Bai, L. Endowing homodimeric carbamoyltransferase GdmN with iterative functions through structural characterization and mechanistic studies. *Nat. Commun.* **2022**, *13* (1), 6617.
(57) Schoenafinger, G.; Schracke, N.; Linne, U.; Marahiel, M. A. Formylation Domain: An Essential Modifying Enzyme for the Nonribosomal Biosynthesis of Linear Gramicidin. *J. Am. Chem. Soc.* **2006**, *128* (23), 7406−7407.
(58) Bai, X.; Chen, H.; Ren, X.; Zhong, L.; Wang, X.; Ji, X.; Zhang, Y.; Wang, Y.; Bian, X. Heterologous Biosynthesis of Complex Bacterial Natural Products in *Burkholderia Gladioli*. *ACS Synth. Biol.* **2023**, *12* (10), 3072−3081.
(59) Niu, W.; Liu, J.; Duan, Y.; Zhong, L.; Pang, L.; Zhong, G.; Zhang, Y.; Bian, X. Biosynthesis of Nonribosomal Peptides Chitinimides Reveal a Special Type of Thioesterase Domains. *Chemistry* **2024**, *30* (69), No. e202402763.
(60) Atik, A. E.; Guray, M. Z.; Yalcin, T. Observation of the Side Chain O -Methylation of Glutamic Acid or Aspartic Acid Containing Model Peptides by Electrospray Ionization-Mass Spectrometry. *J. Chromatogr. B.* **2017**, *1047*, 75−83.
(61) Rüschenbaum, J.; Steinchen, W.; Mayerthaler, F.; Feldberg, A.; Mootz, H. D. FRET Monitoring of a Nonribosomal Peptide Synthetase Elongation Module Reveals Carrier Protein Shuttling between Catalytic Domains. *Angew. Chem., Int. Ed.* **2022**, *61* (48), No. e202212994.
(62) Tanovic, A.; Samel, S. A.; Essen, L.-O.; Marahiel, M. A. Crystal Structure of the Termination Module of a Nonribosomal Peptide Synthetase. *Science* **2008**, *321* (5889), 659−663.
(63) Li, R.; Shi, H.; Zhao, X.; Liu, X.; Duan, Q.; Song, C.; Chen, H.; Zheng, W.; Shen, Q.; Wang, M.; Wang, X.; Gong, K.; Yin, J.; Zhang, Y.; Li, A.; Fu, J. Development and application of an efficient recombineering system for Burkholderia glumae and Burkholderia plantarii. *Microbial Biotechnology* **2021**, *14* (4), 1809−1826.
(64) Chen, H.; Sun, T.; Bai, X.; Yang, J.; Yan, F.; Yu, L.; Tu, Q.; Li, A.; Tang, Y.; Zhang, Y.; Bian, X.; Zhou, H. Genomics-Driven Activation of Silent Biosynthetic Gene Clusters in *Burkholderia Gladioli* by Screening Recombineering System. *Molecules* **2021**, *26* (3), 700.
(65) Thongkongkaew, T.; Ding, W.; Bratovanov, E.; Oueis, E.; Garcı A-Altares, M. A.; Zaburannyi, N.; Harmrolfs, K.; Zhang, Y.; Scherlach, K.; Müller, R.; Hertweck, C. Two Types of Threonine-Tagged Lipopeptides Synergize in Host Colonization by Pathogenic Burkholderia Species. *ACS Chem Biol* **2018**, *13* (5), 1370−1379.
(66) Götze, S.; Stallforth, P. Structure, Properties, and Biological Functions of Nonribosomal Lipopeptides from *Pseudomonads*. *Nat. Prod. Rep.* **2020**, *37* (1), 29−54.
(67) Dose, B.; Niehs, S. P.; Scherlach, K.; Flórez, L. V.; Kaltenpoth, M.; Hertweck, C. Unexpected Bacterial Origin of the Antibiotic Icosalide: Two-Tailed Depsipeptide Assembly in Multifarious *Burkholderia Symbionts*. *ACS Chem. Biol.* **2018**, *13* (9), 2414−2420.
(68) Lin, B.; Hung, A.; Singleton, W.; Darmawan, K. K.; Moses, R.; Yao, B.; Wu, H.; Barlow, A.; Sani, M.; Sloan, A. J.; Hossain, M. A.; Wade, J. D.; Hong, Y.; O'Brien-Simpson, N. M.; Li, W. The Effect of Tailing Lipidation on the Bioactivity of Antimicrobial Peptides and Their Aggregation Tendency: Special Issue: Emerging Investigators. *Aggregate* **2023**, *4* (4), No. e329.
(69) Fu, C.; Keller, L.; Bauer, A.; Brönstrup, M.; Froidbise, A.; Hammann, P.; Herrmann, J.; Mondesert, G.; Kurz, M.; Schiell, M.; Schummer, D.; Toti, L.; Wink, J.; Müller, R. Biosynthetic Studies of Telomycin Reveal New Lipopeptides with Enhanced Activity. *J. Am. Chem. Soc.* **2015**, *137* (24), 7692−7705.
(70) Baltz, R. H.; Miao, V.; Wrigley, S. K. Natural Products to Drugs: Daptomycin and Related Lipopeptide Antibiotics. *Nat. Prod. Rep.* **2005**, *22* (6), 717−741.
(71) Bode, E.; Büllesbach, J.; Bauer, K.; Shi, Y.; Reiners, S.; Cui, Z.; Happel, P.; Shi, Y.; Hoffmann, K.; Grün, P.; Pommerenke, B.; Kazmaier, U.; Grininger, M.; Bode, H. B. Pseudotetraivprolides from Pseudomonas entomophila Provide Insights into the Biosynthesis of Detoxin/Rimosamide-Like Anti-Antibiotics. *Angew Chem Int Ed* **2025**, No. e13287.
(72) Wang, Y.; Qian, G.; Liu, F.; Li, Y. Z.; Shen, Y.; Du, L. Facile Method for Site-Specific Gene Integration in *Lysobacter Enzymogenes* for Yield Improvement of the Anti-MRSA Antibiotics WAP-8294A and the Antifungal Antibiotic HSAF. *ACS Synth. Biol.* **2013**, *2* (11), 670−678.
(73) Ma, G. L.; Candra, H.; Pang, L. M.; Xiong, J.; Ding, Y.; Tran, H. T.; Low, Z. J.; Ye, H.; Liu, M.; Zheng, J.; Fang, M.; Cao, B.; Liang, Z.-X. Biosynthesis of Tasikamides via Pathway Coupling and Diazonium-Mediated Hydrazone Formation. *J. Am. Chem. Soc.* **2022**, *144* (4), 1622−1633.
(74) Liu, Q.; Fan, W.; Zhao, Y.; Deng, Z.; Feng, Y. Probing and Engineering the Fatty Acyl Substrate Selectivity of Starter Condensation Domains of Nonribosomal Peptide Synthetases in Lipopeptide Biosynthesis. *Biotechnol. J.* **2020**, *15* (2), No. e1900175.

https://doi.org/10.1021/jacs.6c01193
J. Am. Chem. Soc. 2026, 148, 9114−9129